MSC THESIS

ASSESSING THE HYDRAULIC CONDUCTIVITY OF THE SEEPAGE-REDUCING MEASURE ‘SAND BENTONITE’ IN DIVERSE ENVIRONMENTS

AUTHOR: J.A. WITTEMAN (JOEP)

DATE : 03RD OF JUNE 2024

Rijkswaterstaat
Ministry of Infrastructure and Water Management

UNIVERSITY OF TWENTE.

COLOPHON

Titel: Assessing the hydraulic conductivity of the seepage-reducing measure 'Sand Bentonite' in diverse environments

Author's details

Author: J.A. Witteman (Joep)

Student number: 2870592

Study: Civil Engineering and Management (CEM)

Profile: Civil Engineering Structures

University: University of Twente

Chair Committee: Prof. dr. K.M. Wijnberg (Kathelijne) (University of Twente)

Daily supervisors: Ir. R. van der Meijden (Rens) (University of Twente)

EngD. A. de Boom (Arthur) (Rijkswaterstaat – GPO)

Date: 03rd of June 2024

Version: Final

PREFACE

This report titled ‘’Assessing the hydraulic resistance of the seepage-reducing measure ZBM in diverse environments’’ represents my master thesis completion as part of my Master of Science in Civil Engineering and Management. The main objective of this thesis was to assess the hydraulic conductivity of ZBM as a seepage reduction measure at the bottom of waterways with varying surface coarseness, pH, and salt concentration of surrounding water. This thesis is commissioned by Rijkswaterstaat-GPO in collaboration with Van Heteren Weg- en Waterbouw B.V. over a period of half an academic year.

I would like to take this opportunity to express my sincere gratitude to the individuals who supported me throughout this journey. Firstly, I am incredibly grateful to Prof. dr. K.M. Wijnberg (Kathelijne) from the University of Twente, who was chair of the committee. Her insights, scholarly wisdom, and guidance were invaluable in shaping the direction of my master's thesis. Additionally, this endeavour would not have been possible without Ir. R. van der Meijden (Rens) and EngD. A. de Boom (Arthur) for their role as my daily supervisors on behalf of the University of Twente and Rijkswaterstaat-GPO. Their mentorship, practical insights, and willingness to share their professional networks were crucial to the success of this project.

I am also thankful to Ing. A. Scheepbouwer (Alex) for sharing invaluable experience regarding conducting experiments and expertise with respect to sand-bentonite on behalf of Van Heteren Weg- en Waterbouw B.V. Furthermore, I would like to express my sincere appreciation to the University of Twente, Rijkswaterstaat-GPO and Van Heteren Weg- en Waterbouw B.V for their support and resources, which have facilitated the completion of this research project.

Joep Witteman, Enschede, May 2024

ABSTRACT

In many regions of the Netherlands, the water level in waterways is higher than the surrounding groundwater level. This water level difference could result in seepage, which could lead to dike failure due to piping or uncontrolled saturation of the soil. Measures such as ZBM (Sand-Bentonite-Mixture or Zand-Bentoniet-Mengsel in Dutch) are applied to mitigate seepage. ZBM is applied as a soft liner at the bottom of waterways, functioning as a poorly permeable layer by increasing the hydraulic resistance and thereby reducing the conductivity. Joint research involving Rijkswaterstaat, Van Heteren Weg- en Waterbouw B.V and Deltares (knowledge institute in water and subsurface) showed that applying ZBM would increase the hydraulic resistance and could confidently be applied as a seepage control measure in the Twentekanaal, which was successfully applied in 2022 and 2023. Following this success, questions arose about whether the ZBM would also be applicable in different environmental contexts.

This thesis assesses the influence of various environmental factors on the hydraulic conductivity of ZBMs used as a seepage control measure on the bottom of waterways. While existing literature offers valuable insights, it often focuses on specific characteristics such as swelling capacity, leaving a gap in knowledge about the factors influencing hydraulic conductivity. This makes it difficult to estimate the influences of the environment on the hydraulic conductivity of the ZBM. By conducting small-scale (5 litre) and large-scale (1000 litre) experiments under various environmental conditions while measuring the water flowing through the ZBM layer, the potential influence of the environment on the behaviour and hydraulic conductivity of the ZBM is assessed.

The environmental factors studied include the coarseness of the surface layer on which the ZBM is applied and the chemical composition of the water in terms of salinity and acidity. Findings indicate that the mixture settles through coarse layers even with very fine gradings, with the separation of lighter and heavier particles observed during settling. Nevertheless, of all the experiments, the lowest discharge trend was observed during large-scale experiments with the coarse surface.

Compared to fresh water, the experiment with water with increased salinity showed that the increased salt concentration accelerated the shrinkage of the ZBM layer, leading to the formation of cracks and increasing hydraulic conductivity. Furthermore, this study revealed the impact of ZBM on the pH of the surrounding water through an exchange of H^+ions that increased the pH of the water to that of the mixture itself.

These results show that the hydraulic conductivity and behaviour of the ZBM can be strongly influenced by environmental factors. This indicates that it cannot be assumed that the ZBM could be applied in all environments, and results from the application of ZBM in other environments are not directly applicable to waterways with different water compositions or soil characteristics. Understanding these influences is critical to ensure the efficacy and applicability of ZBMs in different environmental contexts.

TABLE OF CONTENTS

1. INTRODUCTION

1.1 PROBLEM CONTEXT

In the Netherlands, in many places, the water level in the waterway is higher than the groundwater level in its surroundings. As the water level is higher in the waterway, this induces seepage. Seepage occurs due to differences in water levels between the outer and inner sides of the dike, where water tends to flow from higher to lower water levels through a permeable layer. Seepage induces risks, causing dike failure due to piping or uncontrolled saturation of the soil. Piping could cause internal soil erosion, which causes the soil to be carried out to the exit point. Uncontrolled saturation can lead to rising groundwater levels, resulting in soil instability or flooding. In the Netherlands, various seepage control measures are used, varying from applying low-permeable soil like clay as a liner to sheet piles as underground barriers (Farrar, 2004).

One such measure is ZBM (Sand-Bentonite-Mixture or Zand-Bentoniet-Mengsel in Dutch), introduced by Rijkswaterstaat and Van Heteren Weg- en Waterbouw B.V to address concerns during maintenance dredging and canal deepening at the Twentekanaal. The removal of deposited sludge, which served as a poorly permeable layer, raised the risk of seepage due to the underlying permeable sand layer. The sludge layer increased hydraulic resistance, and its removal reduced this resistance, potentially leading to increased seepage and compromising the stability of hydraulic structures.

To restore hydraulic resistance at the Twentekanaal, Rijkswaterstaat initiated a Value Engineering process, resulting in the application of ZBM. This mixture acts as a soft liner, similar to the removed sludge, providing a poorly permeable barrier. Figure 1 illustrates a simplified representation of a channel where ZBM has been applied. Initially, the poorly permeable layer is partially excavated, reducing hydraulic resistance and causing increased water flow from the canal to the permeable layer, leading to a higher water level on the inner side of the dike. To restore the hydraulic resistance, a 10 cm layer of ZBM is applied at the bottom of the Twentekanaal, which reduces the flow by increasing the hydraulic resistance (Rijkswaterstaat, 2021).

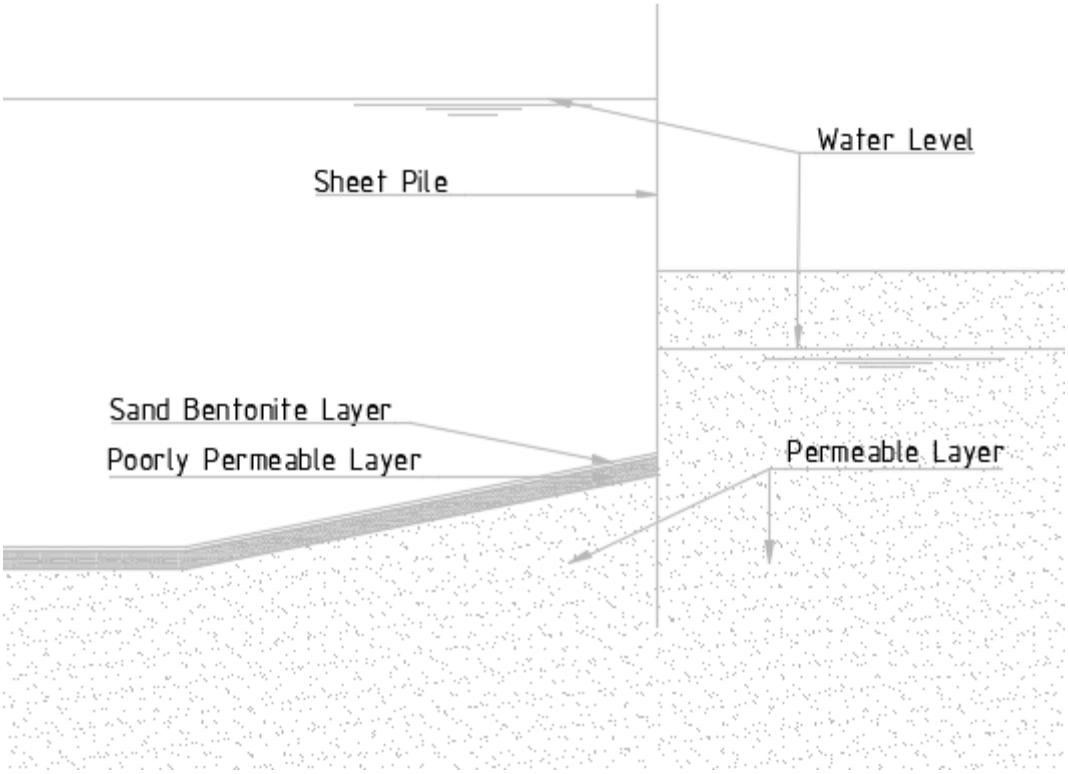

Figure 1, Schematic cross-section canal

When restoring hydraulic resistance, the bentonite particles within the ZBM play a pivotal role, as the ZBM's primary function is to decrease the volume of water flowing from the waterway to its surroundings. To decrease the flow, the bentonite particles infiltrate spaces between sand particles, altering contacts from sand-sand to sand-bentonite. Simultaneously, the seepage-induced suction compacts the ZBM layer, forming a less permeable barrier. These processes collectively impede water flow and increase resistance to seepage by creating stagnant water in micropores due to increased viscosity, effectively decreasing the saturated hydraulic conductivity (Neretnieks et al., 2009; Li, et al., 2020;).

Bentonite possesses a distinctive characteristic, which is the ability to swell. This swelling ability is a response to the attraction of cations and the dipole character of water induced by dissolved precipitated salts, generating a negative surface charge. The swelling ability enables bentonite particles to fill the spaces between sand particles. The swelling process continues until the Critical Coagulation Concentration (CCC) is reached. The CCC denotes the minimum concentration of electrolytes in a suspension at which particles aggregate, initiating the formation of a gel-like substance. Consequently, particle aggregation is influenced by two key factors: the CCC of the bentonite and the salt concentration in its surroundings. Furthermore, the water's pH may potentially impact the bentonite's CCC as the pH of the water becomes below the Point of Zero Charge (PZC). The PZC marks the pH of the transition point at which negatively charged edges become positively charged, facilitating the formation of an edge-face bond, and lowering the bentonite's CCC. Once the CCC is surpassed, the bentonite coagulates, reducing its effectiveness in infiltrating the spaces between sand particles and thereby reducing the ability to create the desired hydraulic resistance (Kim, 2003; Neretnieks et al., 2009; Bae et al., 2021).

In a collaborative effort involving Rijkswaterstaat, Van Heteren Weg- en Waterbouw B.V and Deltares (knowledge institute in water and subsurface), comprehensive research was conducted. This encompassed the production method, implementation techniques, and validation of the ZBM effectiveness. The joint research that was conducted showed that applying ZBM would increase the hydraulic resistance and could confidently be applied as a seepage control measure in the Twentekanaal (Puls, 2020; Talmon & Pennekamp, 2020). Subsequently, in 2022 and 2023, the mixture was successfully applied on a large scale at the Twentekanaal. Based on the outcome of the research and its successful application, the question arose as to whether the ZBM in its current form could also be successfully applied in different environments.

These environmental contexts span variations in physical and chemical conditions. For example, the ZBM might be applied as a seepage control measure near hydraulic structures with low hydraulic resistance and coarse surfaces at the bottom or under the load of river or ship-induced flow and turbulence. Furthermore, it might be employed in saline or brackish environments, potentially affecting the chemical behaviour of bentonite. Assessing the influence of these environmental factors on the hydraulic conductivity is essential to determine whether the mixture could be applied in these situations.

1.2 STATE OF THE ART

ZBM remains relatively unexplored as a seepage control measure in waterways in open contact with surface water. While considerable attention has been directed towards understanding its fundamental properties, such as swelling behaviour, translating these findings directly to hydraulic conductivity poses a significant challenge. The complex interplay of mechanical and chemical factors influencing ZBM behaviour further complicates its practical application.

Research conducted for Rijkswaterstaat has primarily focused on applying ZBM specifically at the Twentekanaal, resulting in limited insights into the influence of varying conditions. Existing literature has focused on specific individual characteristics such as swelling behaviour, but the multifaceted nature of factors influencing ZBM behaviour poses challenges in extrapolating study findings to practical contexts. Although the theoretical understanding of bentonite behaviour is relatively robust, the significant factors vary across experimental setups and mixture compositions, complicating direct comparisons.

This complexity and influence of significant factors are indicated in the study by Prioa et al. (2016), which revealed that the swelling capacity becomes more relevant as the bentonite ratio increases in the ZBM. Furthermore, Dutta & Mishra (2016) observed variations in bentonite quality to affect compression index and volume change. Both these studies highlight the challenges in comparing findings across studies due to the difference in bentonite composition.

Studies investigating the influence of environmental factors on (sand) bentonite behaviour highlight the possible influence of the dissolved solids and water pH. Research by Dutta & Mishra (2016) demonstrated that as the salt concentrations (NaCl and $CaCl_2$) increase, the compressibility, swelling ability and consolidation time decrease while the consolidation coefficient increases. Similarly, Studds et al. (1998) showed that dilute solutions (i.e. low salt concentrations) allow bentonite to swell and separate sand particles under low stresses, while high stresses or concentrated solutions limit swelling to the sand pore volume, affecting the clay void ratio. Furthermore, Alzamal et al. (2021) observed that the chemical composition of synthetic groundwater made using $CaCl_2$, NaCl, and $MgCl_2$ as their main salts significantly reduces swelling potential compared to distilled water. The magnitude of this decrease depends on the volume of total dissolved solids in the solution.

Regarding pH influence, Neretnieks et al. (2009) mention the influence of pH on bentonite behaviour; however, they deem it irrelevant due to the pH conditions of their intended application. According to them, the pH of granitic rocks would not drop below the PZC (point of zero charge) (6.5 to 7) and would, therefore, not influence the bentonite. However, variations in the point of zero charge (PZC) across studies underscore the need for further investigation. For instance, Kim (2003), measured a PZC of 8 using a solubilization technique, suggesting potential impacts on bentonite properties if pH falls below the PZC, which impacts are also indicated by Bae et al. (2021). As prevailing uncertainty regarding pH demands attention, considering that the pH of the water where the mixture might be applied may range from 7 to 8.5 (Rijkswaterstaat, 2024).

In conclusion, as it is apparent that substantial research has been conducted on bentonite, mainly to use as a sealing agent at repository sites, a comprehensive understanding of the influence of environmental factors on hydraulic resistance remains very limited. Additionally, despite the insights, comparing outcomes across studies poses considerable challenges due to the multitude of variables involved, ranging from mixture composition to experimental conditions. The variability in the intended application causes a variety in experimental design, duration, and result interpretation. This creates the need to conduct new experiments tailored to the seepage control setting in waterways.

1.3 PRACTICAL ENVIRONMETAL ASPECTS AFFECTING ZBM

Beyond the chemical environmental factors detailed in existing literature, there are crucial practical environmental considerations that could impact the hydraulic resistance of the ZBM, yet these are not defined in existing literature. These environmental factors include surface type, hydraulic gradient, and river or ship-induced flow and turbulence.

Since there has to be some demarcation of the breadth of this study, only one will be examined. This factor concerns the application of the ZBM on a coarse surface rather than sand. A coarse surface may naturally form due to river deposition or be intentionally created using rubble stones (breuksteen) in waterways to shield against erosion from river or ship-induced flow and turbulence. To cope with this erosion, multiple layers are applied, ranging from fine to coarse, where the coarse layer shields the finer layer from flow and turbulence.

For the mixture to be applicable, the layer must be able to form an interconnected layer, which forms a ‘’blanket’’ to form a poorly permeable layer. However, applying the ZBM on a coarse layer could have a variety of consequences: the mixture could settle on top, settle in between, or settle all the way down until it encounters a layer where it will settle on top. To ensure the formation of an interconnected layer, it is crucial for the mixture to settle as a cohesive unit. However, given the likely heterogeneity of the layer on which the mixture is applied, achieving an interconnected layer may poses a challenge, as different stone gradings may influence behaviour differently. Therefore, gaining insight into the influence of the coarse surface on the behaviour of the ZBM provides insight into its applicability on a variety of surfaces.

1.4 DEFINITION OF THE KEY TERMS

Before defining the research objective and question, it is important to define some key terms and how they relate to the study. These key terms are hydraulic resistance, hydraulic conductivity/permeability coefficient, and volumetric discharge.

The hydraulic resistance can be mathematically explained by Equation 1 and Equation 2. Equation 1 describes Darcy's law, which, in a simplified form, provides an understanding of the key parameters influencing the volumetric discharge. The volumetric discharge is a measure of the total volume of water flowing through the soil per unit time. The volumetric discharge depends on the saturated hydraulic conductivity of the soil, the cross-sectional area of the soil sample, the hydraulic head difference between the inner and outer water level, and the length of the sample layer. The saturated hydraulic conductivity of the soil also referred to as the permeability coefficient, measures how easily a fluid flows through a soil type. The cross-sectional area of the soil sample is the area of which the fluid is flowing through. The hydraulic head difference is the water level difference between the water level at the inner and outer sides of the dike. And the length of the sample is the length of the sample through which the water is flowing. Subsequently, the hydraulic resistance can be calculated using Equation 2 based on the hydraulic head difference, volumetric discharge and cross-sectional area. The hydraulic resistance is a measure of the total resistance exerted by the total package of soil (Nortier & de Koning, 1991; Shaw et al., 2011; Puls, 2020).

$$Q = K_s * A * \Delta h / L \quad (1)$$

$Q = Volumetric\ discharge\ flowing\ though\ the\ sample\ \left(\frac{m^3}{d}\right)$
$K_s = Saturated\ hydraulic\ conductivity\ of\ the\ sample\ (\frac{m}{d})$
$A = Cross\ sectional\ area\ of\ the\ sample\ (m^2)$
$\Delta h = Hydraulic\ head\ difference\ between\ both\ sides\ of\ the\ sample\ (m)$
$L = Length\ of\ the\ sample\ (m)$

Equation 1, Darcy's law (Nortier & de Koning, 1991; Shaw et al., 2011)

$$R = \Delta h / (\frac{Q}{A}) \quad (2)$$

$R = Hydraulic\ resistance\ of\ the\ sample\ (d)$

Equation 2, Hydraulic resistance (Puls, 2020)

As hydraulic resistance, hydraulic conductivity/permeability coefficient, and volumetric discharge are interrelated properties, the influence of the various environments on the ZBM will initially be compared based on the volumetric discharge. Subsequently, as this study aims to contribute to a broader scope in existing literature, the flow through the ZBM layer will be converted to hydraulic conductivity, as this is a commonly used unit in the literature of hydraulic engineering.

1.5 RESEARCH OBJECTIVE

Having identified the factors potentially affecting the hydraulic conductivity of the ZBM, along with the challenges inherent in assessing and comparing its behaviour across different studies, it is essential to clarify that this research does not primarily aim to quantify the extent to which environmental factors affect the hydraulic resistance of the ZBM. Instead, the focus is on qualitatively determining whether various environmental conditions influence the hydraulic conductivity of the ZBM. Providing insights into the potential applications of the ZBM under different environmental conditions. Therefore, the primary objective of this research is:

Assessing the hydraulic conductivity of Sand Bentonite Mixture (ZBM) as a seepage reduction measure at the bottom of waterways with a coarse surface, lowered pH, and increased salt concentration of the surrounding water compared to the Twentekanaal.

1.6 RESEARCH QUESTIONS

As this main objective consists of the coherence of individual environmental factors, research questions are formulated to assess the environmental factors individually. The environmental factors assessed consist of the influence of a coarser surface, increased total dissolved solids (NaCl & CaCl2), and lowered pH compared to those observed in the Twentekanaal.

The defined research questions are:

1. *To what extent does the coarseness of the surface on which the ZBM is applied impact the hydraulic conductivity of the ZBM as a seepage control measure?*
2. *How does exposure to a higher volume of total dissolved solids (NaCl & $CaCl_2$) in the surrounding water compared to the Twentekanaal affect the hydraulic conductivity of ZBMs when used as seepage control measures?*
3. *What is the impact of exposing the ZBM to water with a lowered pH of the surrounding water compared to the Twentekanaal on the hydraulic conductivity of ZBMs when applied as a seepage control measure?*

1.7 OUTLINE

This master thesis is structured into eight chapters and subsequently the references and appendixes.

The first chapter presented the context of the problem and the significance of this study, on which the research objective and questions were based.

In Chapter 2, additional information is presented, providing a deeper understanding of the ZBM and describing how chemical environmental factors theoretically influence the ZBM.

Chapter 3 presents the general research approach, experiment procedure and initial experimental conditions used to assess the influence of the environments on the ZBM. This chapter also describes that the first small-scale experiments are performed as preliminary research for the large-scale experiments, where later on, the answers to the research questions are mainly substantiated on.

The fourth and fifth Chapters provide the results of the experiments. These are divided into Chapter 4, which provides the results of the small-scale experiments, and the large-scale results are presented in Chapter 5.

In Chapter 6, the experimental setups and the observed influence of environmental factors are discussed. This chapter also compares the results of the small and large-scale experiments and how the results relate to that literature.

Chapter 7 addresses the findings based on the research by answering the research questions and the main objective.

Finally, Chapter 8 provides recommendations for practical application based on the identified influential factors. Furthermore, suggestions for future research are proposed to enhance understanding of the factors impacting the ZBM.

2. UNDERSTANDING BENTONITE AND ENVIRONMENTAL INFLUENCES

In this thesis, the understanding of bentonite is primarily based on a literature review that focuses on defining its function; this is done in the first three paragraphs. It starts with briefly describing the origin and structure of the bentonite platelets and subsequently delves into the function of the ZBM as a seepage control measure with a focus on the role of the bentonite. Finally, the processes of the bentonite that cause the swelling are discussed. Thereafter, specific environmental factors that influence the performance of the ZBM will be elaborated on in paragraphs 2.4 and 2.5. These paragraphs link the theory of influential factors to the environmental varieties influencing the characteristics of the ZBM applied as a seepage control measure. The environmental varieties discussed are the influence of the dissolved solids and pH on the mixture.

2.1 ORIGIN AND STRUCTURE

Bentonite, in its raw form, is extracted from mining operations and subsequently dried and processed into either a fine powder or granules. This mineral originates from volcanic ash deposited in enclosed, low drainage areas with high humidity, where the ash is hydrolysed under the influence of water to form silicon (Si^{4+}) and aluminium (Al^{3+}) oxyhydroxides with colloidal properties. Consequently, bentonite primarily comprises the clay mineral known as Montmorillonite, characterised by its unique structure consisting of two tetrahedral layers enclosing an octahedral layer. Figure 2 shows the structure of a Montmorillonite, consisting of two tetrahedral silica sheets within the middle an alumina octahedral sheet (Hofkamp, 1986; Oliveira & Beatrice, 2019).

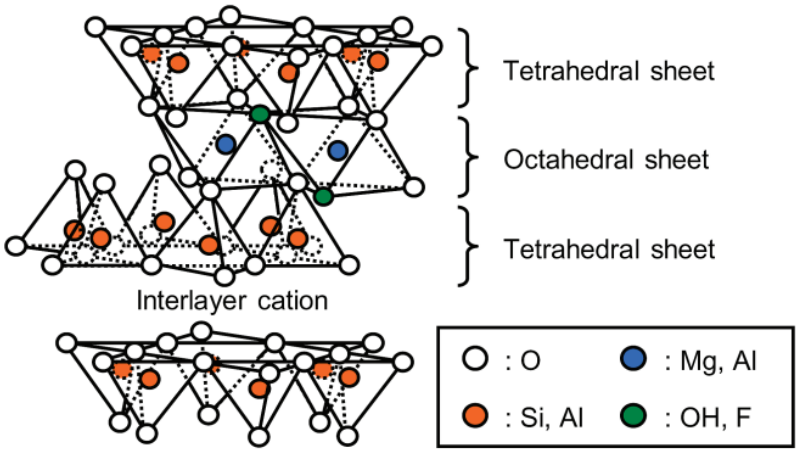

Figure 2, Montmorillonite platelet (Oliveira & Beatrice, 2019)

Within the structure of a Montmorillonite, isomorphic substitution, whereby trivalent ions (Al^{3+}) and tetravalent ions (Si^{4+}) are replaced by divalent ions such as Mg^{2+}, Fe^{2+} and Ca^{2} play a crucial role in the electrical properties of clay minerals. Isomorphic substitution occurs mainly in the octahedral layer and generates negative charges. Consequently, a deficit of positive charges arises within the crystal lattice, leading to an excess of negative charge. This excess is balanced by the attraction of cations present in the surrounding environment, including Na^{+}, K^{+}, Ca^{2+}, and Mg^{2+}, which precipitate onto the exterior surface in the form of salts. As a result, sodium bentonite typically forms in salt-rich environments, while calcium bentonite is more commonly found in a freshwater environment. These exterior cations act as counterions to balance the negative charges after the substitution and are located in interlayer cations (Figure 2) (Bolt & Bruggenwert, 1978; Rehab, 2013; Ghaedi, 2021; Augustijn, 2023;)

2.2 PRACTICAL FUNCTIONING

Before delving further into influential factors, it is crucial to understand the role of bentonite and how the ZBM functions as a liner in waterways to decrease hydraulic conductivity, for example, at the Twentekanaal. In this application, initially, the mixture is created by mixing the bentonite with water, with ratios determined to achieve a desired viscosity of 120 MF, ensuring that the bentonite mixture with water is easily miscible with the sand. Subsequently, fine sand (washed fill sand) is added to the bentonite water mixture, resulting in a mixture consisting of approximately 32% sand, 14% bentonite and 54% water (Puls, 2020).

As the mixture is applied at the bottom of the waterway, it can be described as a colloidal suspension, as fine bentonite is dispersed within the sand in a water mixture. The primary function of bentonite is to mitigate hydraulic conductivity by infiltrating the spaces between sand particles, thereby altering particle contacts from sand-sand to sand-bentonite, as illustrated in Figure 3. This infiltration occurs initially in the macropores, followed by the micropores and nanopores, leading to the expansion of the bentonite. Figure 4 illustrates the microstructure of the bentonite where the nanopores represent the spaces between clay platelets, micropores are situated between clay stacks, and macropores exist between the sand/bentonite pores. The swelling process consists of the subdivision of clay stacks in the micropores and the increase in the spacing between the platelets, reducing the nanopores. These processes are further elaborated on in this chapter (Neretnieks et al., 2009; Li, et al., 2020; Qin et al., 2021).

As the swelling reduces the pores, simultaneously, seepage-induced suction compacts the layer where the mixture interfaces with the underlying sand subsurface. The fine sand lattice undergoes densification compared to its free-moving state in the solution, forming a less permeable layer. Subsequently, the unfilled/ insufficiently filled pores become filled with bentonite as the suction introduces a supply of loose bentonite, filling and clogging the pores. When a barrier is formed by the sand and bentonite, the water becomes stagnant due to the barrier in combination with the increased viscosity due to the attraction of the water particles in the micropores. This significantly impedes the interaction between free-flowing and stagnant water (Neretnieks et al., 2009; Qin et al., 2021; Alzamalet al., 2021).

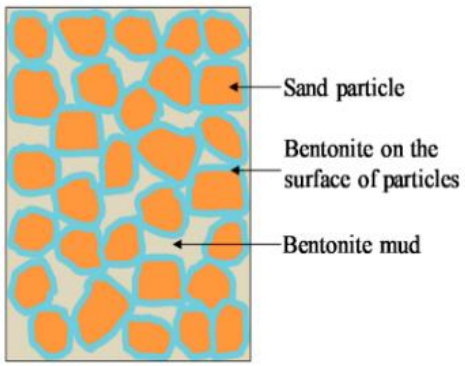

Figure 3, Working mechanism of ZBM (Qin et al., 2021)

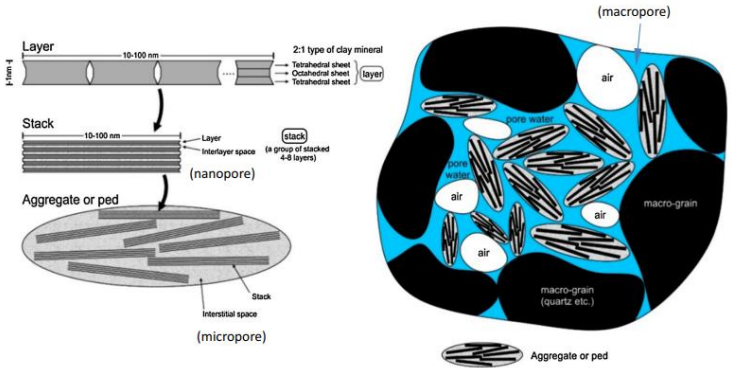

Figure 4, Illustration of microstructure bentonite (Nasir et al., 2017)

2.3 SWELLING MECHANISMS

When exposed to water, precipitated salts at the exterior surface of the clay platelets can dissolve, initiating the swelling of bentonite on multiple scales. The exchange of counterions occurring due to electrostatic forces upon contact with water is expressed as the CEC (Cation Exchange Capacity), referring to the ability of clay platelets to absorb and exchange cations (Neretnieks, Liu, & Moreno, 2009).

On a nanoscale, two types of swelling occur, namely crystalline and osmotic. Crystalline swelling or ''Type I swelling'' is a result of the hydration of the precipitated salts (Na^+, K^+, Ca^{2+}, Mg^{2+}) coupled with hydrogen bonding or charged surface-dipole attraction occurring between the platelets. The conceptual model of this swelling is shown in Figure 5, where hydration takes place in four stages as a result of the attraction of water molecules. This swelling causes repulsive forces between the platelets, mainly caused by the hydration of the interlayer cations, increasing stepwise their distance. This is controlled by a balance between the swelling and the attraction of the adjacent layers (Wayllace, 2008; Christstidis, 2011; Tu, 2015).

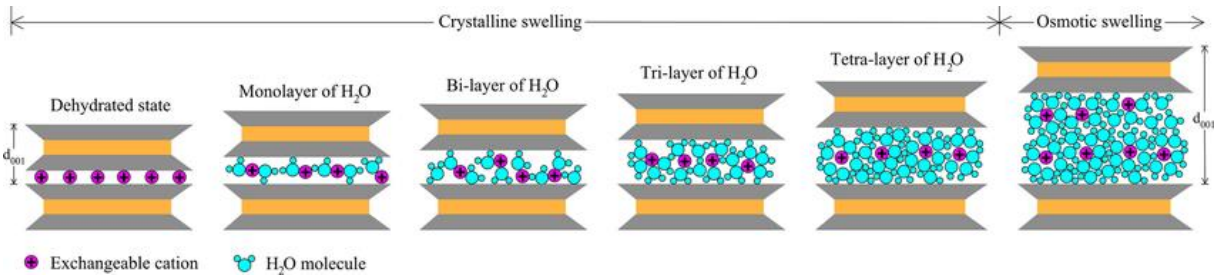

Figure 5, Conceptual model of crystalline swelling (Keerthana & Arnepalli, 2022)

When the interlayer exceeds three to four monolayers of water molecules, the forces related to cation hydration become negligible compared to the electrostatic repulsion. When these are exceeded, the subsequent swelling is referred to as "osmotic swelling". Osmotic swelling is also referred to as ''Type II swelling'' and results from a concentration difference between the dissolved ions between the platelets and the free water around when the negative surface charges attract cations and polar water, as shown in Figure 6 and Figure 7 (Tu, 2015; Alzamal et al., 2021).

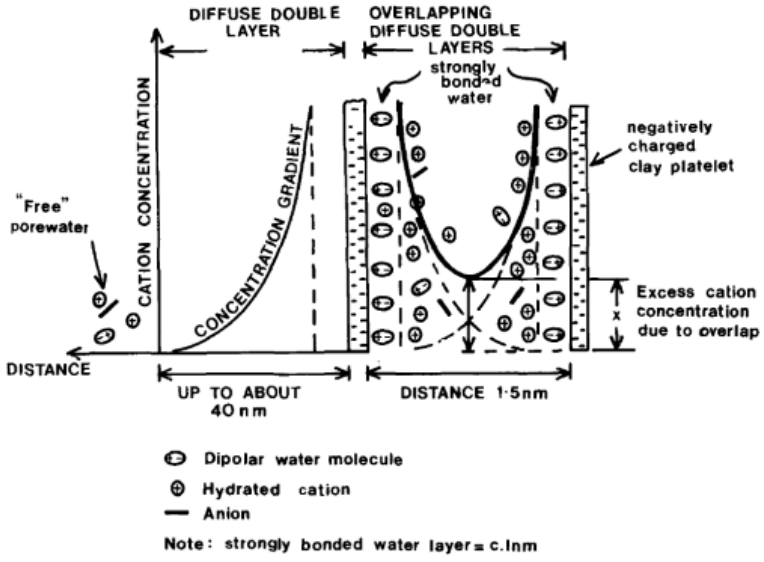

Figure 6, Conceptual model diffuse double layer (Taylor & Smith, 2017)

The attraction of cations and polar water is a consequence of the desire to achieve electrical neutrality near the clay surface. Therefore, the number of cations is relatively large near the clay surface and decreases as the distance decreases as a result of a balance between minimal enthalpy and entropy, while the number of anions decreases near the clay surface, as shown in Figure 6. When the water molecules have a dipole character, they are attracted due to the negative charge of the clay surface. This results in a diffuse double-layer formation when one side of the water molecules is attracted to the negative charge, and the other side tends to diffuse into the solution. The bond between the negative surface and water particles as a result of the diffuse double layer causes the water in the pores of a ZBM to have a greater viscosity, so it moves less freely than free water (Bolt & Bruggenwert, 1978; Studds et al., 1998; Augustijn, 2023).

The attraction of cation by the diffuse double-layer causes a concentration difference that initiates flow from free water to the diffuse double-layer region. The expansion continues until a balance is reached between the concentration of the interlayers and the free water, as seen in Figure 7. Due to the repulsive forces caused by the overlap of two diffuse double layers (Figure 6), the platelets are pushed apart until the concentration of the boundaries of the diffuse double layer is similar to that of the free water (Rehab, 2013; Tu, 2015).

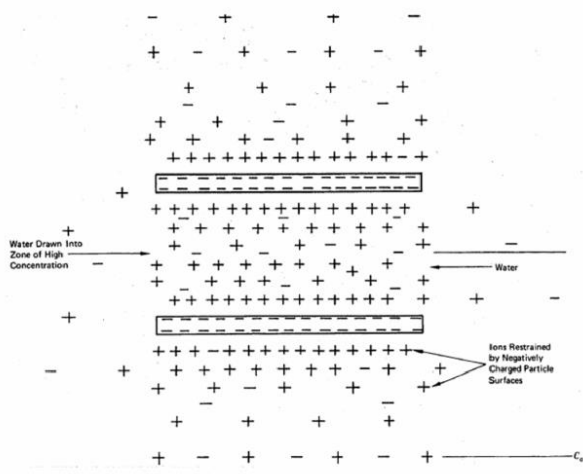

Figure 7, Osmotic swelling between clay platelets (Mitchell & Soga, 1993)

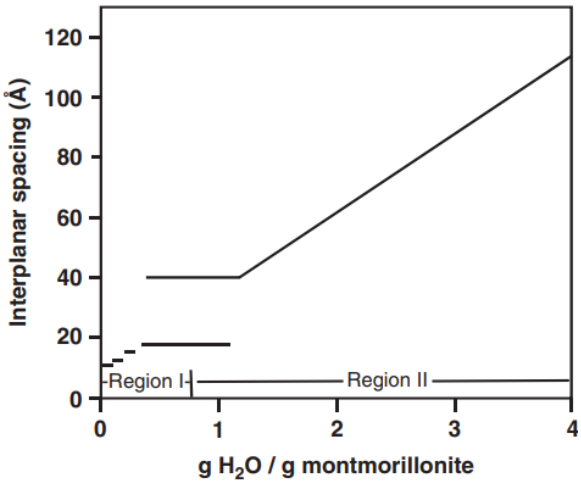

Figure 8, Interplanar spacing crystalline swelling (region I) and osmotic swelling (region II) (Christstidis, 2011)

The extent of crystalline and osmotic swelling in clay minerals is quantified by the CCC (Critical Coagulation Concentration), which denotes the minimum concentration of electrolytes in a suspension required for attractive forces between particles to overcome repulsive forces, resulting in particle aggregation and gel formation. Figure 8 shows the relation between concentration and swelling due to crystalline and osmotic swelling on the distance between platelets. In this figure, it can be seen that osmotic swelling (region II), in particular, results in a notable increase in the interplatelet spacing. When the ion concentration surpasses the CCC, the swelling of bentonite particles halts, and they become a cohesive gel that will not spontaneously release particles. Conversely, if the ion concentration is below the CCC, the particles repel each other due to the diffuse double layer, allowing for continuous swelling (Neretnieks et al., 2009).

2.4 INFLUENCE OF DISSOLVED SOLIDS ON THE BENTONITE

As described in the previous paragraph, two types of swelling fill up the nanopores, namely crystalline and osmotic swelling, which are both influenced by the dissolved solids in the solution. This section will first discuss how the concentration of dissolved solids influences the swelling behaviour of bentonite in a future application as a seepage control measure and, subsequently, the influence of the valency of the dissolved solids.

2.4.1 Influence concentration of dissolved solids

The swelling arises from the attraction of cations as a result of the dissolved precipitated salts at the exterior surface of the clay platelets, which generate a negative surface charge, as previously described in this chapter. These dissolved salts generate a negative layer charge, playing a significant role in the swelling behaviour. The swelling is the result of the balance between the attraction of cations and repulsion between the platelets, caused by the hydration of the interlayer cations and by the diffuse double layer. When the total concentration of dissolved solids is below the CCC (Critical Coagulation Concentration), bentonite continues to swell. Conversely, swelling ceases when the total concentration surpasses the CCC and bentonite particles become cohesive when they no longer repel each other (Neretnieks et al., 2009).

In a situation where the total dissolved solids are below the CCC, this creates a situation where first crystalline swelling occurs and subsequently osmotic swelling. In such a situation, the total dissolved solids determine whether the particles will coagulate and the extent to which the diffuse double layer will diffuse. When the concentration of dissolved solids rises, the diffuse double layer tends to diffuse less due to the greater availability of cations required to neutralise the negative surface charge, reducing the need for further diffusion. This reduction in the diffuse double layer reduces the repulsive forces between the clay particles as the diffuse double layer is thinner, as visualised in Figure 6 and Figure 7 (Neretniekset al., 2009; Christstidis, 2011; Dutta & Mishra, 2016; Alzamalet al., 2021).

During the current process of mixing and maturing the ZBM, the mixture is only exposed to a limited amount of water required to create the correct viscosity. This results in the total dissolved solids being limited during the maturing process, while during the applications, there is a constant supply of dissolved solids as the ratio of ZBM and water during application is negligible over time. Therefore, it is not realistic to assume that the water used for the mixture (54% of the mixture) has the same concentration of dissolved solids as the water where it is finally applied. Without a new supply of dissolved solids, an equilibrium will be reached sooner with a lower concentration of dissolved solids as the attraction of cations reduces the concentration of ‘’free’’ dissolved solids. This process can be described by using Figure 9, which is technically incorrect but illustrates the process. When the mixture is made, the total amount of dissolved water is limited as the only supply of water is the water required for the mixture; therefore, the water will follow the upper track of Figure 9. In this track, the water will first infiltrate the macropores and, subsequently, the micropores. When the water is infiltrated in the micropores, the distance between the clay platelets will start to increase due to the attraction of water molecules due to their dipole character. The concentration of dissolved solids plays a key role in the swelling as the lower the concentration, the larger the swelling, as the bentonite needs to attract more water to create electrical neutrality (Li et al., 2020; Alzamal et al., 2021)

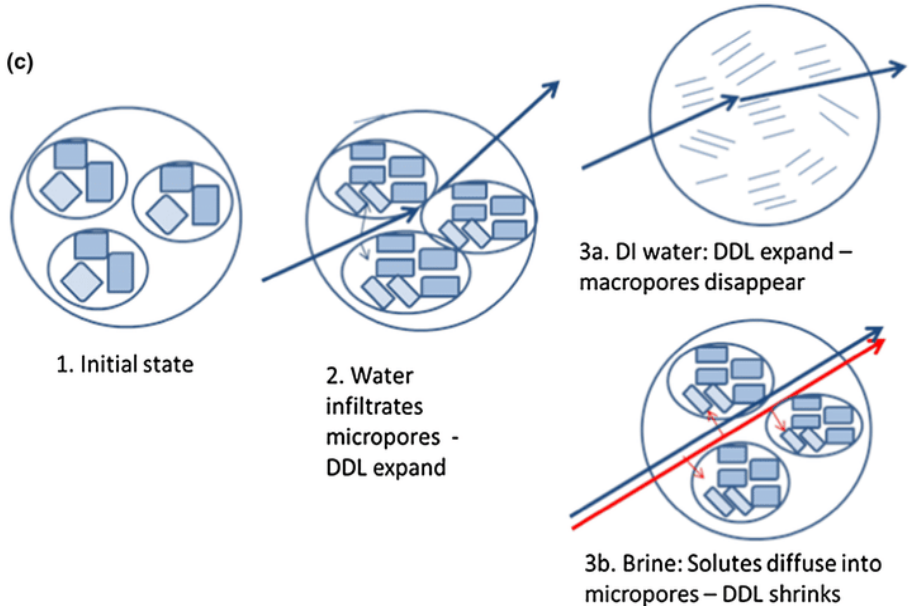

Figure 9, Sequential development of swelling bentonite with water (blue line) and brine (salt water) (red line) (Manca et al., 2015)

Subsequently, when the mixture is exposed to an environment with a constant supply of dissolved solids, this sets a new equilibrium as the concentration of free-flowing dissolved solids will tend to equalise. The simultaneous transport of water and solute in double structures initially causes water to move faster than solute, leading to aggregate expansion. However, the solute gradually migrates into micropores, reducing the swelling and resulting in thicker and denser stacks of platelets until an equilibrium state in a concentration of dissolved solids is reached. This process may take considerable time due to decreased water supply from the low hydraulic conductivity of the sand-bentonite layer. Decreased swelling capacity in practice may hinder bentonite particles from filling macropores as effectively as before, assuming no other processes occur (Li et al., 2020).

The relative concentration of dissolved cations will increase during the application compared to the initial maturing process, as there will be an indefinite water supply with a set concentration of cations. When the relative concentration in dissolved solids increases, this could result in two processes: Firstly, there is a gradual decrease in swelling capacity over time until an equilibrium is reached. This is caused by the fact that there is a higher concentration of cations available to compensate for the negative surface charge and, therefore, a lower width of the diffuse double layer, decreasing the repulsive forces between the platelets. Secondly, the Critical Coagulation Concentration (CCC) may be surpassed as the relative amount of total dissolved solids is higher during application. This could lead to the coagulation of bentonite particles, reducing the ‘’free’’ bentonite particles and reducing the ability to clog up the pores. Both processes require time for the "new concentration" to diffuse into the pores and for the bentonite to react; accordingly, therefore, these processes will not be observable directly (Neretniekset al., 2009; Li et al., 2020).

2.4.2 Influence of valency of dissolved solids

In addition to concentration, the valency and, therefore, the type of cations also influence bentonite swelling ability. A solution with higher valency cations can lead to the exchange of bivalent and trivalent cations with monovalent (sodium ions) ones due to the greater affinity of higher valency cations, affecting bentonite behaviour. In the current application, sodium bentonite is used, thus susceptible to exchange by higher valency cations, potentially impacting long-term behaviour. Contact with solutions containing high concentrations of divalent cations, such as calcium ions, results in ion exchange, with calcium ions replacing sodium ions bound to clay mineral surfaces until equilibrium is reached. The concentration of the dissolved divalent or trivalent ions controls the rate and extent to which the ion exchange occurs and could even cause a reversal of the exchange reaction (Christstidis, 2011; Dutta & Mishra, 2016; Kong et al., 2017).

Initially dominated by sodium, sodium ions with lower ionic strength result in repulsive forces outweighing attractive ones, enhancing swelling capacity and CCC. However, the replacement of sodium ions with calcium ions of higher ionic strength leads to attractive forces outweighing repulsive ones (illustrated in Figure 10), causing the particles to aggregate and increase cohesion. Calcium-dominated bentonite forms denser and more cohesive gels, as CCC of calcium bentonite only permits crystalline swelling. As the CCC is dependent on several factors and varies in the literature, Neretnieks et al., (2009) state that ''When the pore waters contain more than about 50 mM monovalent cations, give or take a factor of 2, the smectite gel is cohesive and does not release individual particles by Brownian motion. For calcium, only about 1 mM is needed to generate a cohesive gel.'' This indicates the significant difference in CCC between sodium and calcium bentonite (Neretnieks et al., 2009; Alzamalet al., 2021).

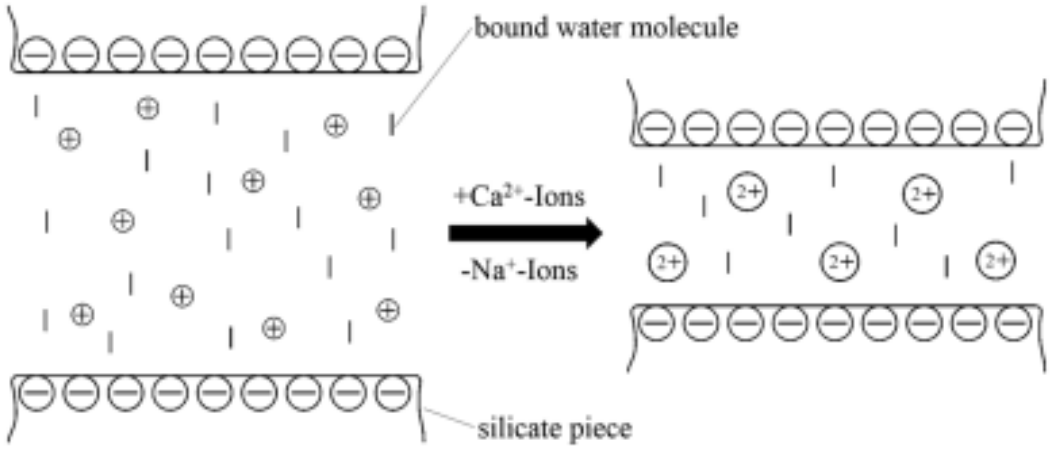

Figure 10, Exchange of monovalent sodium ions for divalent calcium ions (Kong, Wu, Chai, & Arulrajah, 2017)

Moreover, as sodium-dominated bentonite transforms into calcium-dominated platelets, they tend to combine into compact stacks, reducing volume. This results in decreased bentonite volume and an inability to release particles, potentially negatively affecting the ability to clog the pores and self-healing (Neretnieks et al., 2009; Alzamalet al., 2021).

Sand-bentonite's future application will likely be in freshwater environments with a higher calcium/sodium ion ratio compared to its initial composition during mixing/maturing. The exchange of these sodium ions will likely impact hydraulic conductivity as characteristics gradually shift towards those of calcium bentonite. Driven by the stronger affinity of higher valency cations, it can lead to a reduction in Critical Coagulation Concentration (CCC), thereby triggering the coagulation of bentonite particles. This coagulation is a result similar to that caused by the increase in total dissolved solids described in the previous paragraph, where the CCC is also exceeded. However, in this case, the CCC is lowered, and the concentration for the surrounding water to exceed the CCC could be reached with lower concentrations of total dissolved solids (Neretniekset al., 2009).

It must be noted that according to Neretnieks et al. (2009), before sodium bentonite will start to behave like calcium bentonite, approximately 90% of the charge-compensating ions must be calcium ions, with fewer calcium ions, the bentonite will behave more like pure sodium bentonite. This is in case the bentonite originates from pure sodium bentonite. However, for this application, the bentonite originates from calcium bentonite, which is transformed into activated sodium bentonite using soda ash. This conversion process introduces a degree of unpredictability due to incomplete sodium-for-calcium ion exchange and a possible higher affinity for calcium ions. This may influence the transformation point at which the behaviour shifts from sodium to calcium bentonite (Christstidis, 2011).

2.5 INFLUENCE OF THE PH ON THE BENTONITE

Until now, only a negative surface charge has been described as a result of the dissolved solids; however, positively charged edges could also occur under specific conditions, as their electrostatic charge is pH dependent. The clay platelets possess a permanent charge, which remains unaffected by the pH of the surrounding aqueous environment; however, they also possess a non-permanent, pH-dependent charge. This non-permanent charge results from the uptake or removal of H^+ ions at the edges of the platelets, as illustrated in Figure 11. At low pH, the surface charge may shift to positive due to H^+ ion uptake, whereas at high pH, H^+ ion removal results in a negative change (Christstidis, 2011).

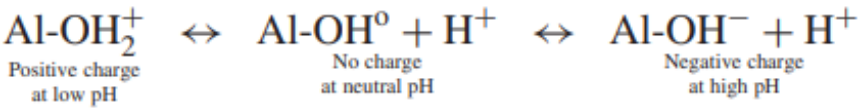

Figure 11, Schematic representation of uptake and removal of H^+ ions aluminol (Christstidis, 2011)

The turning point from which the negatively charged edges become positively charged is called the PZC (point of zero charge). It is worth noting that the exact value of the PZC varies in the literature, ranging from 6.5 to 10. In Kim's (2003) study, where the PZC was measured using a solubilisation technique, a PZC with a pH of 8 was observed for bentonite. Although the permanent charge of smectites remains constant, the non-permanent charge fluctuates with changes in pH, influencing their overall charge properties. However, this influence on the overall surface charge is often considered negligible due to their significantly greater length compared to width (Kim, 2003; Augustijn, 2023).

A process with greater relevance is that the positively charged edges could form an edge-face bond between the positive edges and negative faces. The extent and rate of this phenomenon remain uncertain due to limited research, particularly in comparable compositions and applications. In a situation where the pH is below the PZC and in combination with a high salt concentration, this could result in the diffuse double layer tending to diffuse less far and get somewhat compressed. Furthermore, this could lead to an interaction between the edges and flat surfaces of the particles, causing them to stick together (aggregation). This causes a decrease in CCC, which results in a lower maximum swelling capacity and an increase in cohesion. Conversely, at pH values above the PZC, both the flat surface and edges are negatively charged, resulting in stronger repulsion between particles, stabilising the suspension and increasing CCC (Neretnieks et al., 2009; Bae et al., 2021).

As this thesis aims to assess ZBM's applicability in various environments, the pH of future possible applications could vary depending on the location, and even at a location, the pH could fluctuate, as shown in Appendix I (Table 12). This table shows quartiles and averages of the measured pH and the number of observations from 2013 to 2022. Over the 22 locations, almost all averages are slightly below the PZC (pH 8), underscoring the importance of assessing whether pH levels below 8 will affect ZBM performance/hydraulic conductivity across various locations (Rijkswaterstaat, 2024).

Overall, despite the uncertainty surrounding the pH of the PZC and the extent to which it exerts influence on the CCC of the bentonite, the pH remains a point of attention. Over time, it is reasonable to expect that the lower pH of the surrounding environment will gradually cause the pH of the ZBM to decrease until it aligns with its surroundings. When the pH of the bentonite drops below its PZC, the potential for an edge-to-face bond arises, lowering the CCC. When the total dissolved solids' concentration surpasses the bentonite's CCC due to a lowered CCC, the bentonite will stop swelling or even decrease in swelling, and the bentonite starts coagulating.

3. RESEARCH METHODOLOGY

3.1 GENERAL APPROACH

Since this subject of the master thesis is relatively unexplored, the nature of this study is exploratory, gaining knowledge by performing experiments. The research methodology comprises two small-scale experiments and one large-scale experiment. This division allowed for partial simultaneous execution, leveraging insights from small-scale experiments to large-scale experiments. A visualisation of the research structure is shown in Figure 12.

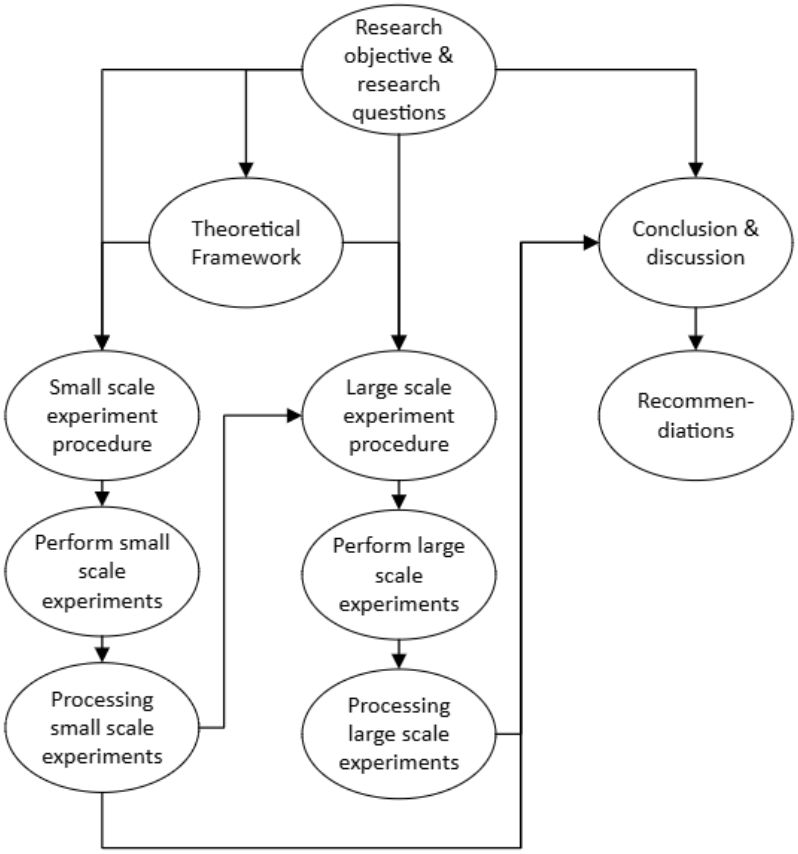

Figure 12, Visualisation of the research structure

The small-scale experiments were set up as accessible and simple as possible to make experimenting as easy as possible due to the large number of desired experiments. These experiments were directly based on the research questions with the objective of gaining desirable knowledge to serve as a foundational understanding for the subsequent large-scale experiment. Moreover, these small-scale experiments reduced the number of large-scale experiments that needed to be carried out, as the first insights had already been gained on a smaller scale. This division facilitated efficient time utilisation. An overview of the experiment is given below:

1. Small-scale experiment with a coarse surface: this experiment aimed to enhance the understanding of how surface coarseness impacts the ZBM's hydraulic conductivity and provides insights into its settling behaviour (research question 1).
2. Small-scale experiment with saline and lowered pH: this experiment aimed to understand the influence of a saline environment and a lowered pH on the hydraulic conductivity of the ZBM (research questions 2 and 3).
3. Large-scale experiment: this experiment aimed to confirm trends observed during the small-scale experiments and to generate insights to answer the three research questions individually.

3.2 EXPERIMENTAL RESOURCES AND MEASUREMENTS

The primary resources and measurements that apply to all experiments, regardless of the scale, are briefly elucidated here. These resources and ways of measuring were kept constant throughout the experiments. Starting by outlining the key resources, namely the ZBM, sand, and water, followed by an explanation of the pH and electrical conductivity measurement methods.

A consistent batch of ZBM, provided by Van Heteren Weg- en Waterbouw B.V, was used throughout the experiments, containing a volumetric sand concentration of 26%. This batch of ZBM was made using the same facility that supplied the mixture for the Twentekanaal and was very similar to the mixture used in the study of Puls (2020), where the ZBM contained a sand concentration of 25%. The bentonite is activated sodium bentonite, referred to as OCMA powder from the supplier CEBO and the sand in this mixture is fine-washed fill sand (CEBO , 2024).

The sand used during the experiments to simulate the bottom surface was very coarse sand (crusher sand), having a size range from 0 - 4 mm. This type of sand presented an unfavourable situation due to its relatively large pores and high permeability.

For the water, it was not possible to use the same type throughout all the experiments due to the two experiment locations. The tap water used for the small-scale experiments originated from the province of Utrecht, and the water for the large-scale experiments is softened tap water from Overijssel. For all experiments, tap water was used unless noted differently, where, in some cases, substances were added to increase the salinity or lower the pH.

Furthermore, the water's pH and electrical conductivity (EC) were measured during all experiments except for the small-scale experiments with the coarse surface. During this experiment, the focus was on the settling and not the chemical influence of the coarse surface on the water or ZBM. The pH is a negative logarithm of the concentration of hydrogen ions, which was measured using a pH test using drops, which quantifies pH in increments of 0.5 units. The EC is a measure of the total number of ions dissolved in the water. The EC was measured using an electrode, which in this case ranges from 0 to 19,900 µS/cm with an accuracy of 100 µS/cm. The samples for the measurement were taken at the surface of the water (Augustijn, 2023).

3.3 SMALL-SCALE EXPERIMENT WITH A COARSE SURFACE

3.3.1 The procedure of the experiment

This small-scale experiment focused on applying the ZBM on a coarse surface. The primary objective of this experiment was to enhance the understanding of whether surface coarseness impacts the ZBM's hydraulic conductivity and provide insights into its settling behaviour. Ideally, this experiment aimed at selecting the coarseness of the surface layer for the large experiment at which the mixture could settle within or on top of the coarse surface layer to form a poorly permeable layer.

Given this study's exploratory nature, the stones' coarseness was not predetermined based on a normative scenario. Instead, a diverse range of gradings was selected to provide a comprehensive understanding of coarseness influence. In this experiment, the influence of the surface layer coarseness was assessed by applying the ZBM onto various grading stones, simulating various surfaces. The behaviour of the ZBM was assessed visually, and the discharge was measured. To better estimate the influence of the applied mixture, the discharge of the coarse surface is measured both with and without ZBM, making it possible to isolate the impact of the mixture on the discharge of the coarse surface.

For the small-scale experiments, a 5-litre measuring cup was used to perform the experiments; a plastic measuring cup was chosen because of its transparency and readability. At the bottom of this measuring cup, a hole was drilled at which a hose was attached; at the end of this hose, a bucket with an overflow was positioned to collect the effluent.

The experiment was performed in four steps:

1. A layer of stones equivalent to 3 litres (13.5 cm) is placed in the measuring cup. Prior to the experiment, the stones were rinsed as cleanly as possible to prevent clouding of the water in a later stage of the experiment.
2. In the second step, the water was added up to the 4.5-litre indicator while the bucket was at the same height as the measuring cup to prevent the test from starting due to a water level difference. An overview of the setup at the second stage is shown in Figure 13.

Figure 13, Small-scale experiment coarse surface – Experimental setup, second step, filling up the measuring cup up to the 4.5 litre indicator

3. In the third step, a 0.9 litre ZBM was applied on top of the stones, which equals 3.8 cm of ZBM. The choice of this specific amount was twice the contents of the used bottle (bottle with a wide opening due to the relatively high viscosity of the mixture), and based on insights at that moment, it would be sufficient for a sealing layer. Before the mixture was applied, it had to be ensured that the ZBM was well mixed to ensure a homogeneous mixture. During the application, the mixture was applied as carefully as possible by using a funnel to prevent the clouding of the water and to apply it as evenly as possible.
4. In the last step, the bucket was lowered, initiating water flow. In the bucket, an overflow is located around 55 cm below the bottom of the measuring cup when lowered. Immediately after the bucket was placed on the ground, 5 litres of water were added carefully using a second measuring cup (left cup Figure 13). The discharge of the surface layer was compared based on the drainage time for the 5-litre volume.

3.3.2 Initial experimental conditions

To better understand the influence of a coarse surface on the discharge and the settling behaviour, experiments were performed with a wide variety of gradings. The experiment was performed with seven different surfaces, from which an overview is shown in Table 2. For this experiment, the largest grading was 50-140 mm, as this was the upper limit the setup could facilitate.

Table 1, Initial conditions for the small-scale experiment coarse surface – Size range coarse surfaces

Type	Size range (mm)	
Caldurite	2	8
Walloon Limestone	8	16
Gravel	16	32
Greywacke	11	56
Limestone (track ballast)	30.5	50
Basalt (rubblestone)	50	140
Coarse sand	0	4

3.4 SMALL-SCALE EXPERIMENT WITH SALINE AND LOWERED PH

3.4.1 The procedure of the experiment

During this experiment, the focus was on providing a better understanding of whether a saline environment or a lowered pH would influence the hydraulic conductivity of the ZBM. These tests had a duration of 10 days; while longer durations would be ideal, a balance was struck between experiment duration and the number of experimental variations.

This experiment used a similar setup to the other small-scale experiment. However, the water was added to the measuring cup when it ran dry instead of measuring the time it would take for 5 litres to drain through the layer during this experiment.

The influence of the saline and lowered pH was assessed visually and by measuring. The measuring which took place consisted of daily determining the water level. By subtracting the water level from one day to the next, the discharge was determined. Additionally, the pH and EC were measured. This was done for the influent at the start and for the effluent each time the measuring cup was refilled and at the end of the experiment. Furthermore, a picture of the ZBM layer was taken daily, making it possible to compare the behaviour of the mixture over time with respect to …

The experiment was performed in the following four steps:

1. The base layer was built up and consisted of a layer of gravel (16-32 mm) up to approximately the 1.5-litre mark (7.5 cm) with 1 litre (4.5 cm) of coarse sand on top; the coarse sand simulated a worst-case scenario as it replicated a very permeable bottom. The first layer of gravel was applied to prevent the hose from clogging up or being blocked. Additionally, below the gravel and between the gravel and sand, a piece of geotextile was located. Geotextile is highly permeable but acts as a barrier for the sand to prevent the hose from clogging up or being blocked. A preview of the layer built-up is shown in Figure 14.

Figure 14, Small-scale experiment saline and lowered pH – Layer build up

2. The specific water was added to the measuring cup after being prepped first. The water was prepared in a 5-litre measuring cup where the specific amount of pH minus or salt was weighed up to prepare 4 litres of water with the right concentration. Subsequently, the water needed to be mixed well to ensure a uniform mixture for this experiment; this was done using a drill with a sufficiently long mixer. After the water was mixed, the pH and electrical conductivity were measured, and the mixture was carefully poured into the measuring cup to prevent the sand layer from becoming uneven up to the 4-litre mark. Important to note is that during this step, the overflow in the bucket needed to be at the same height as the water level in the measuring cup to prevent flow before the start of the experiment.
3. In the third step, 0.9 litres of the ZBM were applied on top of the sand, similar to the small-scale experiment with the coarse subsurface. This causes the water level to increase to the 4.9-litre mark or just below it, as seen in Figure 14.
4. Then, similar to that of the small-scale experiment with the coarse surface, as the layer build-up was completed, the bucket next to the measuring cup was lowered 55 cm to the ground, initiating flow. The outflow of the measuring cup was determined by reading the water level on the measuring cup. The scheduled times to read the water level were set on a daily basis till the measuring cup ran dry. After the cup ran dry, it was refilled with the same water as the experiment started.

3.4.2 Initial experimental conditions

During this experiment, tests were performed to determine whether key characteristics, such as the pH and dissolved salts, would influence the hydraulic conductivity of the ZBM. As this experiment was exploratory, the chemical composition of the water was not based on normative scenarios. In some scenarios, the chemical composition was also somewhat extreme compared to reality, with the idea of accelerating the processes within a relatively short ten-day duration and compensating for the ZBM buffering characteristic.

An overview of the pH and EC of the water used during the experiment is shown in Table 2. For this experiment, the water to which pH minus and salt (NaCl) were added consisted of tap water from the region Utrecht. pH minus was added to lower the pH, which is a solution used in aquariums to lower the water pH. To achieve a pH of 6.5, 0.5 ml/l pH minus was added, and for the 5.5, 1 ml/l was added. Furthermore, fine table salt (NaCl) with a concentration of 5 g/l and 30 g/l was added to the water to create a saline environment. An experiment was also conducted with demineralised water as demineralised water is (almost) free from any dissolved solids. This experiment would indicate if the hydraulic conductivity of the ZBM layer was sensitive to dissolved solids.

Table 2, Initial conditions for the small-scale experiment saline and lowered pH – pH and EC of the influent

	pH (-)	EC (µS/cm)
Tap water	7.5	300
Demi water	6	0
pH 6.5	6.5	300
pH 5.5	5.5	400
NaCl (5g /l)	7.5	7900
NaCl (30 g/l)	7.5	>19900

3.5 Large-scale experiments

3.5.1 The procedure of the experiment

The large-scale experiments were performed to fulfil two objectives: the first, to confirm trends observed during the small-scale experiments, and the second, to generate insights and knowledge for answering the research questions. It must be noted that during this experiment, the applied layer of ZBM had a thickness of 10 cm instead of 3.8 cm during the small-scale experiment. This was chosen because the large scale provides the possibility of applying a thicker layer, and 10 cm is similar to the actual thickness applied at the Twentekanaal and in the experiments of Puls (2020). This increases the comparability of the measurements and observations of the experiment with the results of the study by Puls (2020).

The setup consisted of two similar IBC containers (cubic barrels), as shown in Figure 15. These two containers are identical except for the sight glass in one of the two containers, which was used to observe the behaviour of the ZBM from the side. The influence of the sight glass is expected to be negligible. The top of both containers was cut open to make it possible to apply the layers, and they were filled by a toilet valve, ensuring a constant water level throughout the experiments. This water level was kept constant at 0.5 meters above the applied ZBM layer. The container's bottom had an outlet, which, on the inside, was connected to a 3.5-meter drain incorporated within the sand layer and connected to the outflow of the IBC container. This drain prevented sand from clogging the outflow and impacting test results. At the outside, the outlet was connected via a hose to an overflow system, preventing air from entering the filter package.

Figure 15, Large scale experiment - Setup overview

Figure 16, Large scale experiment – Mortar containers placed on scale

Each experiment was performed with a duration of at least 22 days, which was expected to be sufficient to provide first insights into how the different environmental factors affect hydraulic conductivity. However, as circumstances allowed it, the duration of the first round (reference and coarse surface) experiments was extended to 26 days. And the experiments with the added NaCl were shortened as it ended on the 18th day due to the high discharge values.

The water from the overflow was collected in a mortar container of 65 litres placed on top of a scale (Figure 16). This container was weighted manually daily except during the weekends and public holidays. It must be noted that the collection of water started 30 minutes after the outlet valve was opened, which was opened simultaneously with the application of the ZBM. As during the application of the ZBM, the discharge through the effluent obtained distortedly high values as initially the surface was not covered with ZBM.

Additionally, alongside measuring the outflow, parameters such as water pH and EC were measured at three moments during the experiment. First, at the start, the inflow, water in the IBC container, and effluent for the first half hour were measured. The second moment was on day 14 or 15, when the water in the IBC container and the effluent from that day were measured. The third moment was at the end of the experiment when the water in the IBC container and the effluent from the last day were measured.

Furthermore, visual inspections were included to assess the top layer of the ZBM on the possible formation cracks and the disconnection between the ZBM layer and the container's edge. Also, at the end of the experiment, during the removal of the ZBM, samples were collected from the ZBM layer using an electrical tube. In each experiment, three samples were taken from different locations to assess the layer build-up of the ZBM and its uniformity.

The experiment was performed in the following three steps:

1. A layer of 30 cm coarse sand is added to the container, mimicking the subsurface. After the sand was added, the container, including the sand, was thoroughly rinsed, and compacted to prevent clouding and settling of the sand layer during the experiment. If the experiment was conducted with a coarse surface layer, an extra layer of 35 cm stones was added, as the application is shown in Figure 17 and the final layer build-up in Figure 18.

Figure 17, Large-scale experiment – Applying a coarse layer on sand subsurface

Figure 18, Large-scale experiment - Coarse surface layer build-up (35 cm)

2. After the sand was rinsed well (checked via the clarity of the effluent), the desired water level was marked. Subsequently, an extra mark was set 10 cm below the desired water level to which the water would be filled. This lower mark indicates a volumetric addition of 10 cm of ZBM when the water level increased from the lowest to the upper mark. At the end of this step, the water was levelled to this lower mark, and the outlet closed, ensuring a stable water level. Notably, the water used during this step depends on the desired environment to be assessed.
3. Third, the ZBM was added; therefore, the mixture was first poured over in a container strapped on a pallet where a hose with two nozzles located 2 meters below the container was used for the application, replicating a pressure similar to conditions during the application at the Twentekanaal as shown in Figure 19 and Figure 20. At the end of this hose, a distribution piece distributes the mixture to two nozzles 10 cm apart, which place the mixture as carefully as possible at the surface, as shown in Figure 20. Simultaneously with the application of the mixture, the valve of the outflow below the container was opened.

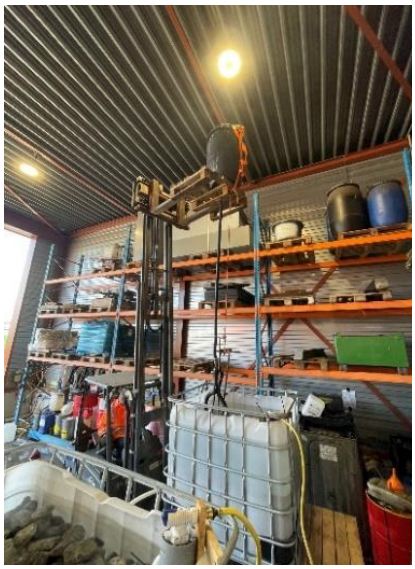

Figure 19, Large scale experiment - ApplicatiorFigure 20, Large scale experiment – Applying ZBM underwater close up method

3.5.2 Initial experimental conditions

The large-scale experiments were performed to better understand the influence of the various environmental conditions and to confirm the trends observed during the small-scale experiments. Five experiments were performed, varying in their initial conditions, but all with an initial ZBM layer of approximately 10 cm. The experimental conditions included a reference case, coarse surface, saline environment (NaCl & $CaCl_2$) and lowered pH, which was similar to those of the small-scale experiments except for the experiment with $CaCl_2$, which was added. $CaCl_2$ was added to the experiments as new insights were gained with respect to the possible influence of higher valency cations. An overview of these initial conditions is shown in Table 3.

Table 3, Initial conditions for the large-scale experiment – pH and EC of the influent

	pH (-)	EC (µS/cm)
Tap water	7.5	400
Coarse surface	7.5	400
pH lowered	6.0	900
NaCl (8g/l)	7.5	15000
$CaCl_2$ (0.64 g/l)	7.5	1300

The first experiment was performed with softened tap water from the Van Heteren Weg- en Waterbouw B.V site located in Hengelo. The second experiment was performed with conditions similar to the first; however, before the ZBM was applied, a coarse layer of 35 cm of rubble stones was applied. These rubble stones (Ardenner grijs) ranged from 45 to 80 mm. This coarseness was chosen as the small-scale experiment showed that regardless of the coarseness, the ZBM would settle on the sand sublayer, and the grading would have a minimal influence on this settling. Therefore, this 45-80 mm seemed to be the best trade-off between real-world applicability and handling ability during the tests.

The initial conditions for the third to fifth experiments were based on historical data reflecting normative scenarios, with detailed substantiation provided in Appendix I. The third experiment was performed with a lowered pH of 6.0, the fourth with a sodium chloride concentration of 8 g/l and the fifth with a calcium dichloride concentration of 0.64 g/l.

4. RESULTS SMALL-SCALE EXPERIMENTS

4.1 RESULTS OF THE SMALL-SCALE EXPERIMENTS WITH A COARSE SURFACE

4.1.1 Overview results

During this experiment, the objective was to enhance the understanding of whether surface coarseness impacts the ZBM hydraulic conductivity and provide insights into its settling behaviour. This was done by measuring the time it would take for 5 litres of water to pass through the ZBM layer and by visual observations. The measured time is shown in Table 4 for the situation without and with the applied ZBM layer. This table shows no value for the sand with ZBM, as the drainage time was significantly longer. The following paragraphs contain the observations for the coarse (stone) surface and sand separately, as the ZBM behaved very differently when applied to the sand surface compared to the coarser gradings.

Table 4, Small scale experiment coarse surface - Timed drainage of 5 litres

	Time (sec)	
	Without ZBM	**With ZBM**
Caldurite	00:35	00:39
Walloon Limestone	00:34	00:36
Gravel	00:33	00:34
Greywacke	00:32	00:36
Sand	01:14	-

4.1.2 Influence coarse surface

Starting with the behaviour on the coarse surface, these experiments showed that even before the bucket was placed on the ground to create drainage, the ZBM had already sunk into the voids in between the stones. As seen in Figure 21, 0.9 litres of ZBM were applied on top of 3 litres of stones, whereby the mixture immediately ran down through the void during application. Therefore, the experiments with the two largest gradings were not continued after applying the ZBM, as the ZBM would run down and clog up the drain. For the four remaining stone gradings, drainage times for 5 litres of water were measured both without and with the ZBM to discern potential differences in subsurface influence. An overview of these results is shown in Table 4. This table shows that all types of stone gave comparable results where, in all cases, the time increased with the applied ZBM. However, the observed difference is negligible, and it can be concluded that applying the mixture atop the stones does not create a poorly permeable layer in the experimental setup utilised.

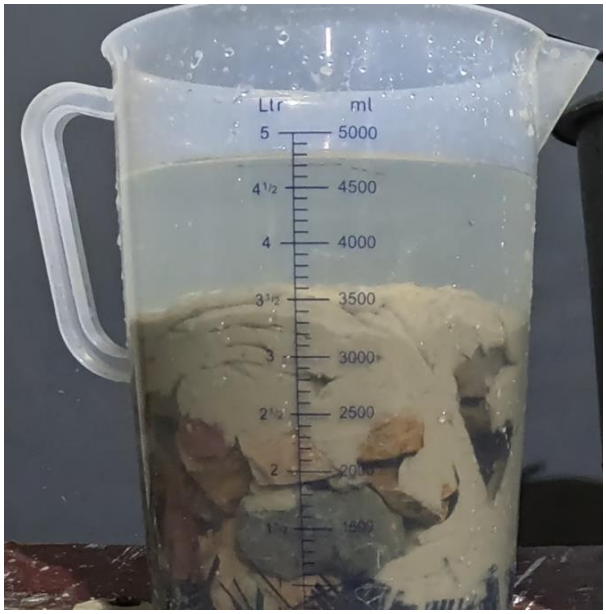

Figure 21, Small scale experiment coarse surface - Greywacke 11-56 mm before drainage

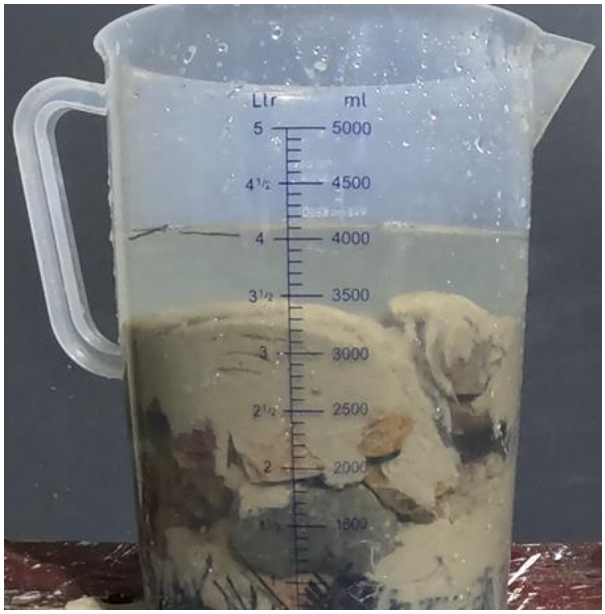

Figure 22, Small scale experiment coarse surface - Greywacke 11-56 mm after drainage

Furthermore, the visual observations aligned with the timed measurements, confirming that, although the ZBM initially remained on top (shown in Figure 23) after the five litres of water were drained, most of the mixture had already settled downwards through the stone layer (Figure 24), being unable to form a poorly permeable layer. This took place to such an extent that it is expected that if more water would be drained, the mixture would likely settle on the layer below the coarse layer.

Figure 23, Small scale experiment coarse surface - Caldurite 2-8 mm before drainage

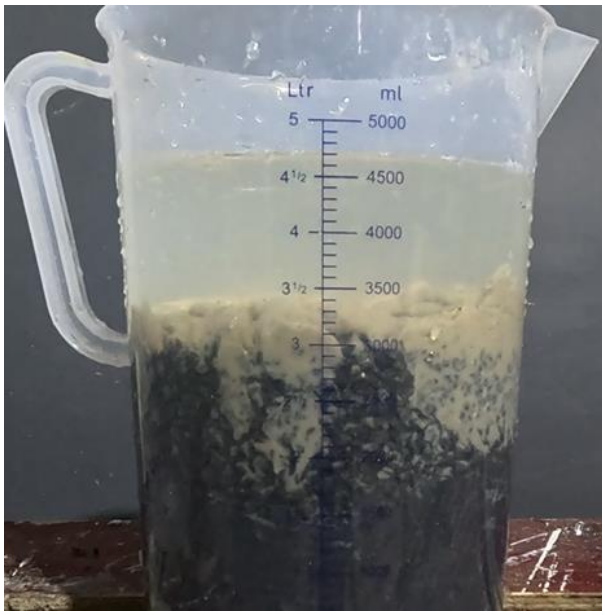

Figure 24, Small scale experiment coarse surface - Caldurite 2-8 mm after drainage

4.1.3 Influence sand surface

Additionally, applying the ZBM on top of the sand surface showed its ability to form a poorly permeable layer. Where without applying the ZBM, the sand layer already achieved the longest time of 1:14 minutes to discharge five litres of water, equating to a hydraulic conductivity of 230 m/d. After applying the ZBM on top of the sand, the mixture immediately created a poorly permeable layer, resulting in almost no drainage. This is displayed in Figure 25 and Figure 26. In Figure 25, the ZBM was applied on top of the sand, whereas in Figure 26, the water level is shown 10 minutes later, with no water added, indicating a significantly longer drainage time compared to the coarse surfaces.

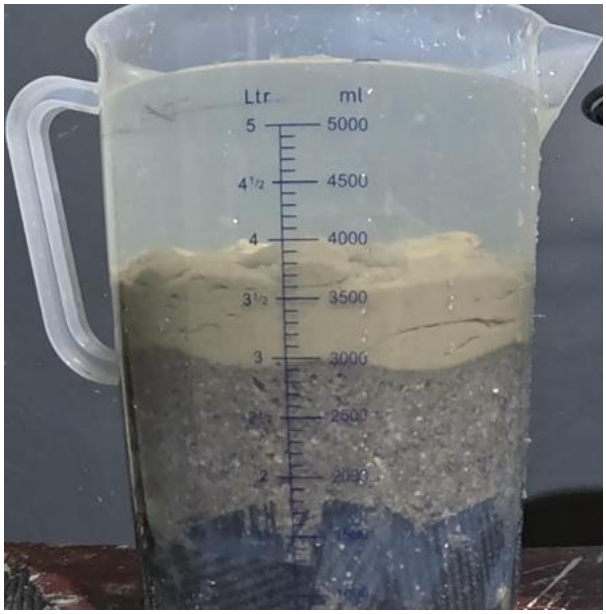

Figure 25, Small scale experiment coarse subsurface - Coarse sand before drainage

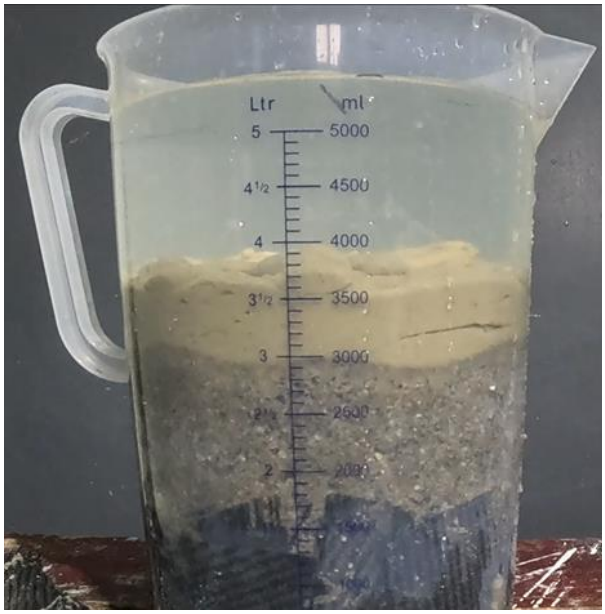

Figure 26, Small scale experiment coarse subsurface - Coarse sand after drainage

4.1.4 Key findings

This experiment aimed to enhance the understanding of how surface coarseness impacts the ZBM's behaviour and provide insights into its settling behaviour. The experiment showed that regardless of the coarse layers applied, the ZBM would settle through the layer and was unable to settle on top or within the coarse layer. These insights were included in the setup of the large-scale experiment by taking the possible settlement into account in advance. The large-scale setup would allow the settlement through the coarse layer until it reached a finer layer.

4.2 RESULTS SMALL-SCALE EXPERIMENT WITH SALINE AND LOWERED PH

4.2.1 Overview results

The pH and electrical conductivity (EC) of the various concentrations during the experiment are shown in Table 5. In this table, the influent is the water used during the start of the experiment. The effluent is the water from the drain, which passes through the ZBM layer. The pH and EC were measured at the end of each experiment. Additionally, if the water had to be topped up during the test, this was done with the same water that the test started with and the pH and EC of the effluent at the time of topping up was measured. After this measurement, the bucket containing the effluent was emptied. Notably, the measuring cup containing water with added salt concentration did not run dry.

Table 5, Small scale experiment - EC and pH of the influent and effluent

	Influent		**Effluent**				
			First refill			**End**	
	pH	**EC**	**pH**	**EC**	**Day**	**pH**	**EC**
Tap water (ref)	7.5	300	7.5	400	4	8	400
Demi water	6	0	7.5	400	6	8	500
pH 6.5	6.5	300	8	400	2	8	800
pH 5.5	5.5	400	7.5	600	6	8	800
NaCl (5g /l)	7.5	7900	-	-	-	8	5800
NaCl (30 g/l)	7.5	>19900	-	-	-	8	>19900

During this experiment, the discharge shown in Figure 27 is determined by the water level difference from one day to the next, divided by the time difference between the measurements, and subsequently converted to a daily unit per square meter to enable comparison with the large-scale experiments. This is necessary as not every daily measurement took place at the same time. Whereas the total discharge in Figure 28 is the sum of the discharge in Figure 27. Furthermore, in Figure 27 and Figure 28, the arrows pointing down indicate the moments of refill and arrows pointing up the observations of cracks. For clearance, the arrows indicating the refill indicate refilling up to the 5-litre indicator.

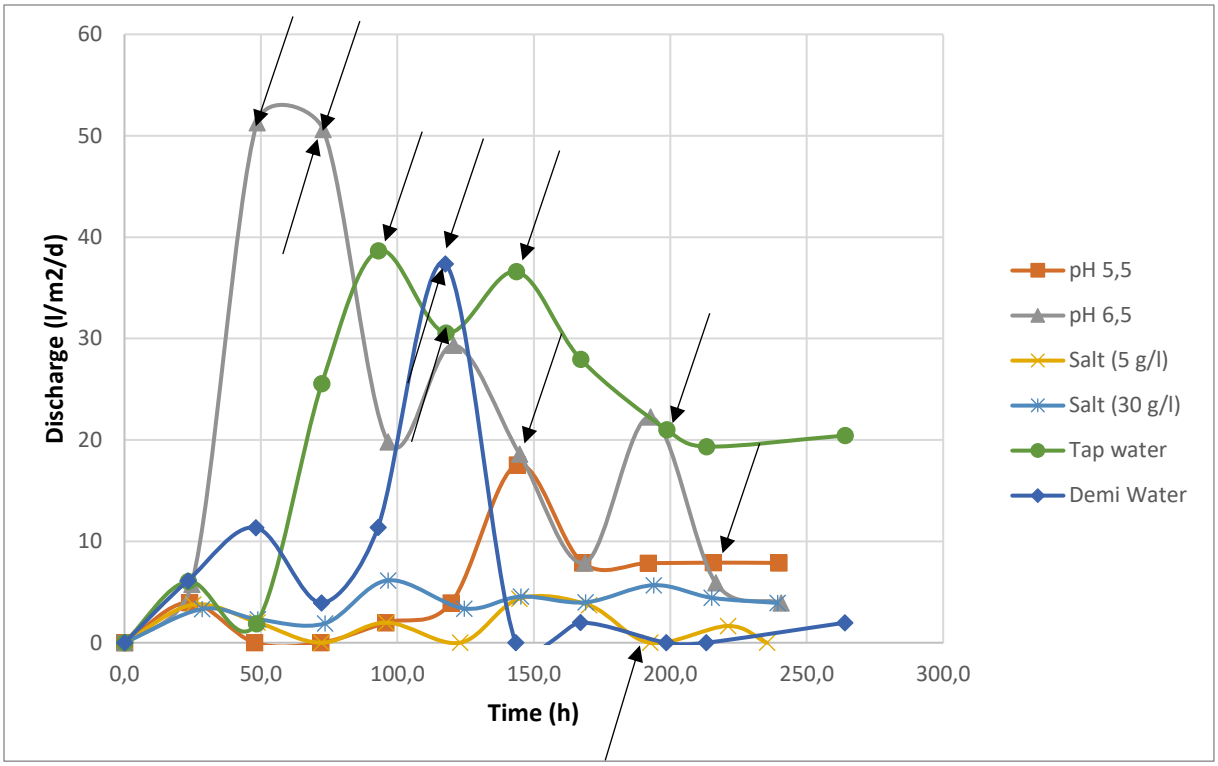

Figure 27, Small scale experiment - Discharge in various environments, arrows pointing down indicating the moments of refill and arrows pointing up indicating the moment of observation cracks

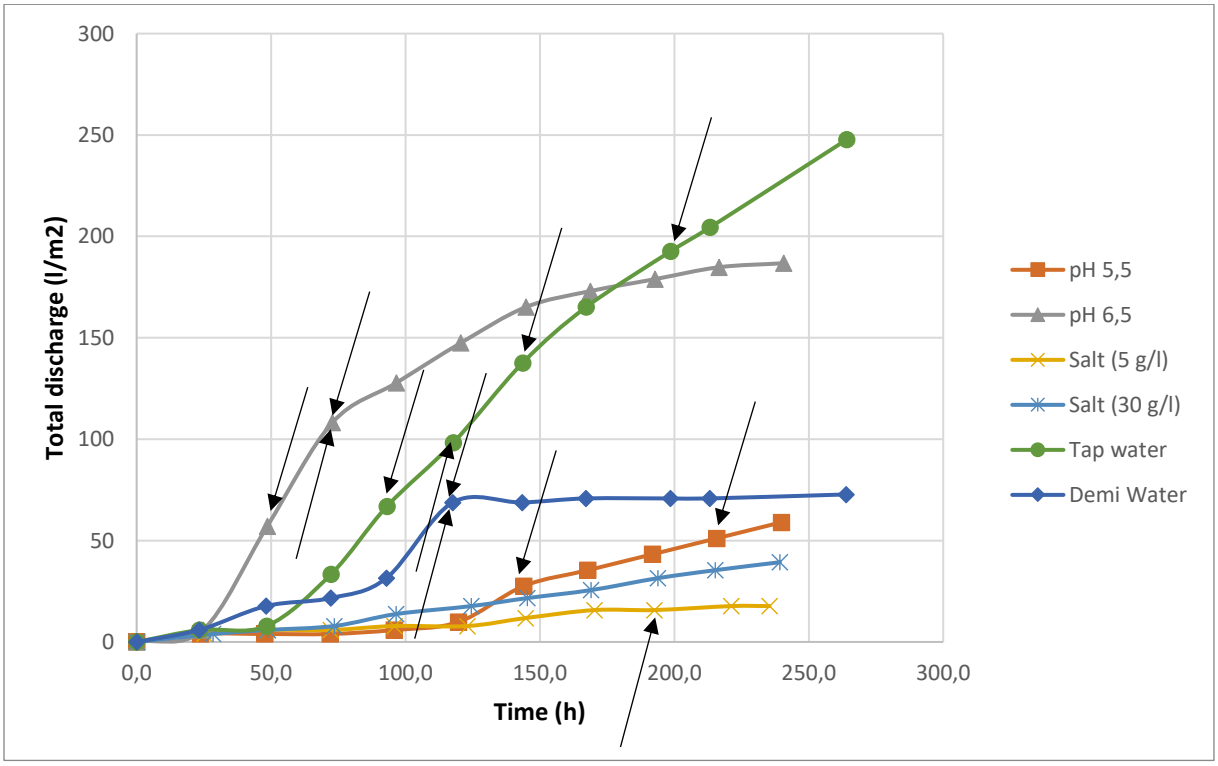

Figure 28, Small scale experiment - Total discharge in various environments, arrows pointing down indicating the moments of refill and arrows pointing up indicating the moment of observation cracks

4.2.2 Tap water (reference)

The experiment with tap water acts as a reference case. Beforehand, the water had a pH of 7.5 and an EC of 400, whereas over the course of the experiment, the pH increased to 8, and the EC remained at 400.

During the first days of the experiment, the discharge was relatively low, but it increased on day 3; from this day onward, the discharge remained above 20 l/m²/d with no signs of a possible decrease. In total, 6300 ml passed through, which is equivalent to a total discharge volume of 247.7 l/m². On the fourth day, the measuring cup was refilled as 1700 ml had passed through, and the measuring cup ran dry. On the fifth day (178 hours), a crack occurred (Figure 29); however, this crack was minimal, and no direct effects on the discharge were observed.

Figure 29, Small-scale experiment saline and lowered pH - Tap water on day 5

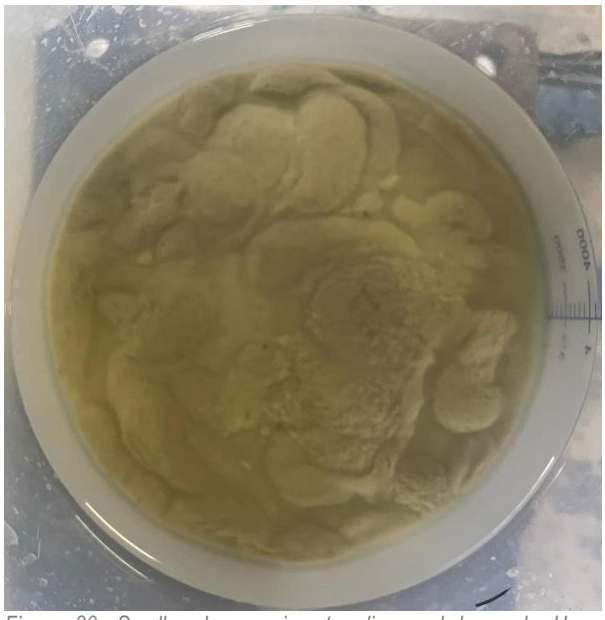

Figure 30, Small-scale experiment saline and lowered pH - Demineralised water on day 4

4.2.3 Demi water

An additional experiment was conducted using demineralised water. Demineralised water does not contain dissolved ions and normally has, after distillation, a pH of 7. However, prior to the test, the water used had a pH of 6, which may be because it is older demineralised water. Nevertheless, the EC was 0, as expected. Following the first refill, pH and EC increased to 7.5 and 400, respectively, with final values reaching pH 8 and EC 500.

During the first days, the discharge fluctuated with the highest discharge of 11 l/m²/d, whereas on day 5 (118 hours), the discharge peaked (37 l/m²/d). After the peak in discharge on the fifth day, it decreased drastically. Between the sixth and eleventh days, the total discharged volume was 100 ml, which is equal to 4 l/m² in five days. Altogether, this resulted in a total discharge volume of 1850 ml, equal to 72.7 l/m²/d.

On the fifth day after the peak in discharge, the water was refilled with demineralised water. During this experiment, it was notable that the water remained significantly more clouded, even after refilling. Furthermore, a visual difference in the ZBM surface layer was observable as the layer looked fluffier, and the application pattern was hardly visible, as shown in Figure 30.

4.2.4 Saline

The experiment in a saline environment was performed with two initial salt concentrations, consisting of an added salt (table salt) concentration of 5 and 30 grams per litre in the tap water, both starting with a pH of 7.5. The addition of 5g/l yielded an EC of 7900, while 30g/l resulted in an EC exceeding 19900, the limit of the measurement device. By the end of the experiment, both concentrations reached a pH of 8, with the EC of the 5g/l concentration decreasing to 5800 and still remaining above 19900 for the 30g/l concentration.

The discharge in both cases remained in the same order of magnitude during the course of the experiment without any extraordinary fluctuations, and no formation of cracks was observed. Overall, the low discharge resulted in a total discharge volume of 450 ml (18 l/m²/d) for the 5 g/l added salt and for the 30 g/l added a total of 1000 ml (39 l/m²). Furthermore, during the experiments, the application structure remained visible for both salt concentrations, as shown for one of the concentrations in Figure 31.

Figure 31, Small-scale experiment saline and lowered pH - Saltwater (30 g/l salt) on day 5

Figure 32, Small-scale experiment saline and lowered pH - Acidic water (pH 6.5) on day 4

4.2.5 Lowered pH

During this experiment, the initial water was lowered to a pH of 6.5 and 5.5 with an EC of 300 and 400. In total, the water with an initial pH of 6.5 was refilled three times, and the water with a pH of 5.5 was only refilled once. As the water was topped up, the pH and EC were measured, resulting in a higher pH and EC of the effluent than the influent. Namely, the pH of 6.5 increased in two days to 8 and an EC of 400, whereas the pH of 5.5 increased to 7.5 and an EC of 600 on the sixth day. At the end of the experiment, the pH was 8 and EC 800 for both cases.

The experiments showed significantly different values for the discharge. The water with an initial pH of 6.5 showed a peak in discharge on the second (49 hours) and third day (73 hours), which was the highest discharge measured (>50 l/m²/d) compared with the other small-scale experiments. Over time, this discharge decreased. The other experiment with a pH of 5.5 showed relatively low and constant discharge, except for one peak of 18 l/m²/d on the sixth day (144 hours).

For the experiment with the initial pH of 6.5 the start of the formation of cracks was notable on the third day, as shown in Figure 32. These cracks remained visible and stable throughout the experiment without new cracks appearing. In total, a total discharge volume of 4750 ml (187 l/m²) had passed through, and for the water with an initial pH of 5.5 a total discharge volume of 1500 ml (59 l/m²).

4.2.6 Key findings

This small-scale experiment aimed to provide a better understanding of the influence of lowered pH and increased salt concentration (NaCl) on the discharge through the ZBM. Table 6 provides an overview of the most important observations. Volumetric units in the table are converted to square meters to facilitate comparison with larger-scale experiments and existing literature.

The hydraulic conductivity in Table 6 was calculated using Equation 1 of Chapter 1. Where for the discharge volume, the median discharge was used. Direct measurements for both the hydraulic head difference and sample length were not taken during the experiment; therefore, these values were derived from other measurements. The hydraulic head difference was determined by measuring the distance from the average water volume in the measuring cup to the ZBM, resulting in a difference of 6 cm. The sample length was estimated by multiplying the ZBM layer thickness during application by the average settlement ratio observed in large-scale experiments, resulting in a length of 2.23 cm.

Table 6, Small scale experiment – Key findings, overview results

	Duration	First Occurrence of cracks	Lowest discharge	Highest discharge	Median discharge	Total discharge	Variation coefficient	Hydraulic conductivity
Unit	***days***	***day***	***l/m²/d***	***l/m²/d***	***l/m²/d***	***l/m²***	***-***	***10^{-3} m/d***
Tap water	11	5	1.89	38.65	23.28	247.7	0.50	8.85
Demi water	11	5	0	37.35	2.96	72.74	1.46	1.13
pH 6.5	10	3	3.94	51.28	18.62	186.76	0.78	7.07
pH 5.5	10	-	0	17.55	5.91	58.98	0.84	2.25
NaCl (5g /l)	10	8	0	4.35	1.82	17.69	0.94	0.69
NaCl (30 g/l)	10	-	1.91	6.15	3.95	39.32	0.32	1.50

From Table 6, it becomes clear that the discharge can vary significantly, reflected in the hydraulic conductivity. Both tap water and water with a pH of 6.5 exhibited significantly higher discharge volumes, whereas water with 5g/L salt added showed a notably lower discharge volume and, thereby also a lower hydraulic conductivity.

The varying values for the discharge make it difficult to draw conclusions for the large-scale experiment. However, visual observations suggest an influence of dissolved salts. The demineralised water test highlighted the impact of a lack of dissolved ions on mixture behaviour, as the water remained cloudy, and its texture appeared fluffier. In contrast, adding salt demonstrated the influence of excess ions, resulting in a more cohesive structure indicated by a recognisable application structure. This detailed structure was not observed in the other experiments. Furthermore, crack formation varied between experiments, suggesting it was not directly correlated with the discharge. Tests with lowered pH suggested that the ZBM influenced the water, as the pH quickly increased during the experiment, rather than the pH affecting the ZBM.

5. RESULTS LARGE-SCALE EXPERIMENTS

5.1 OVERVIEW RESULTS

Table 7 shows an overview of measured EC and pH during the experiment. In this table, the influent is the water initially mixed, which was later pumped into the IBC. The IBC indicates the water which is exposed to the ZBM in the container above the mixture. The effluent is the water from the outflow collected in the mortar container. This table shows that while the pH of the effluent throughout the experiment increases, the EC remains stable throughout the experiment except for the added salt concentrations, which showed some fluctuations in the EC.

Table 7, Large scale experiments - EC and pH of the influent and effluent

	Influent		Start				Day 14/15				End			
			IBC		Effluent		IBC		Effluent		IBC		Effluent	
	pH	EC	pH	EC	pH	EC	pH	EC	pH	EC	pH	EC	pH	EC
Tap water	7.5	400	8.5	400	8.5	400	8	400	8	400	7.5	400	8	500
Coarse surface	7.5	400	8	400	8.5	500	8	500	8	500	8	500	8	400
pH 6	6	900	6.5	900	8	600	8	700	8	800	8	700	8	800
NaCl (8 g/l)	7.5	15000	8	15200	8	6500	8	12200	8.5	11500	8.5	8700	8.5	11900
$CaCl_2$ (0.64 g/l)	7.5	1300	7.5	1700	8.5	900	8	1100	8.5	1200	8	900	7.5	1400

In Figure 33 and Figure 34, the discharge and total discharge are shown after the first half hour of the experiment has passed. The first half hour has not been taken into account due to the temporary high initial discharge (up to 1150 l/m²/d). In both these figures, the arrows indicate the first observation of the formation of cracks, which were only observed for the added salt concentrations.

The discharge in Figure 33 is determined by dividing the difference in discharge volume by the difference in time and subsequently converting it to a 24-hour time scale. The discharge is only determined for the cases where an observation was taken one day before. This resulted in the fluctuation in discharge over the weekend, and Monday could not be observed. The total discharge in Figure 34 is the course of the sum discharge volume, which was also collected at the weekends; however, it was only measured on the following working day, making it unable to determine the daily discharge at the weekends and public holidays.

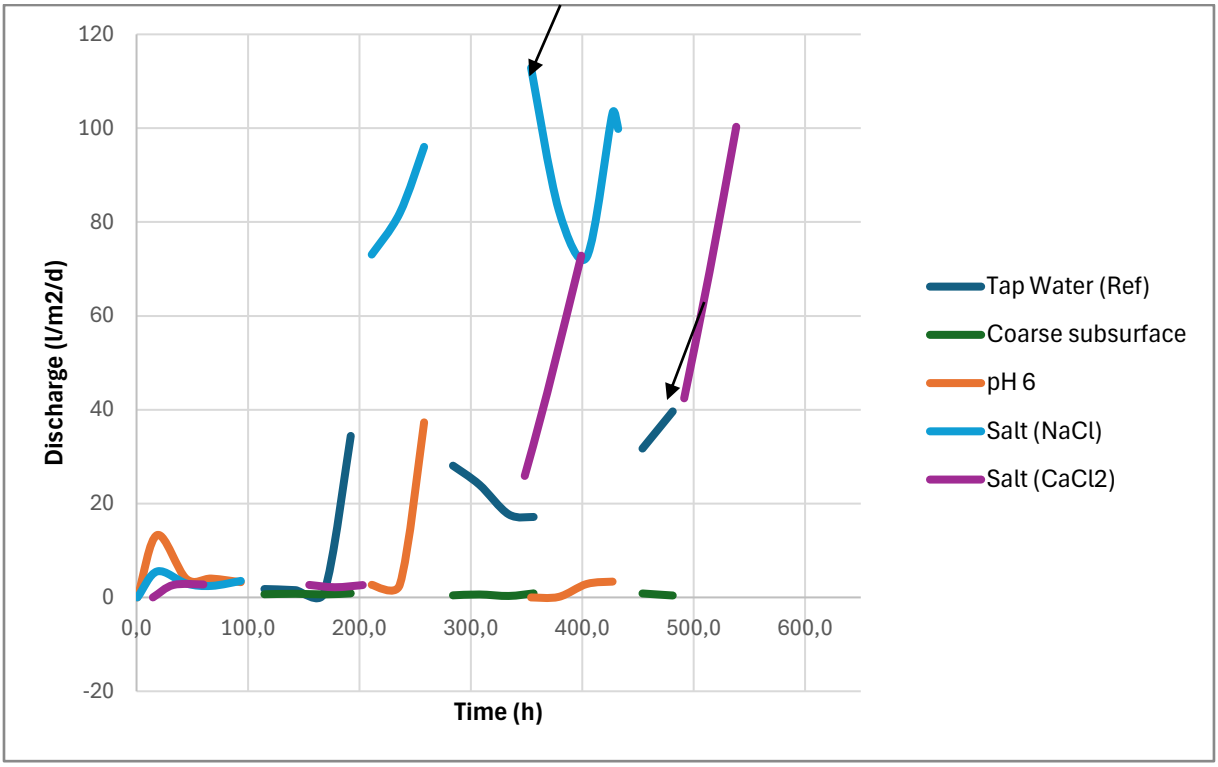

Figure 33, Large scale experiment - Discharge in various environments, arrows indicating the moment of observation cracks

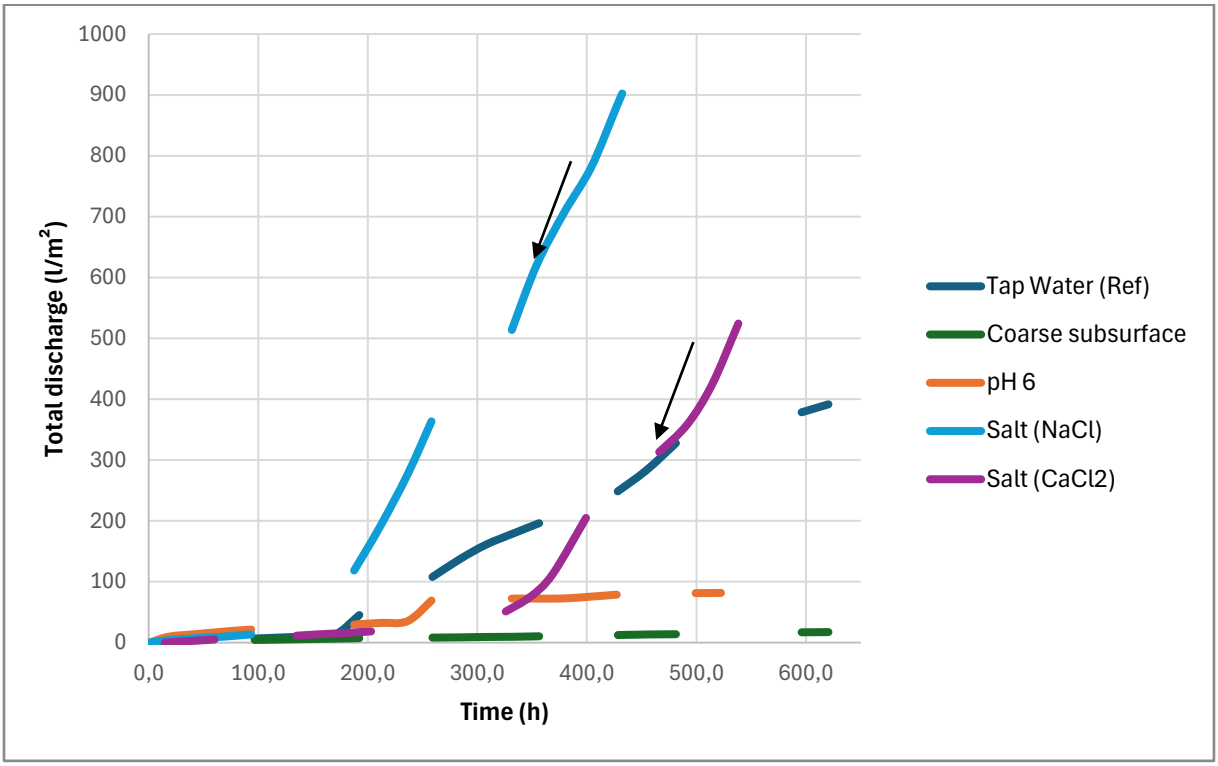

Figure 34, Large scale experiment - Total discharge in various environments, arrows indicating the moment of observation cracks

5.2 TAP WATER (REFERENCE)

In the first round of the large-scale experiments, experiments were performed with tap water and a coarse surface. Starting on January 18th, it took place 26 days and went on until February 13th. As a result of the application of the ZBM, the water remained clouded until the eleventh day, when slowly, due to assumably settlement, the ZBM layer became visible.

On the 13th day, it became visible that the ZBM layer had detached from the tank near the corner of the tank, as can be seen from the photograph taken on the 18th day shown in Figure 35. This detachment was not able to heal itself during the test. Furthermore, it is unclear whether this had already occurred earlier due to the presence of the fluffy/densely clouded layer on top, which made it impossible to observe the ZBM layer.

Figure 35, Large scale reference - Layer became loose on February 5th

Figure 36, Large scale reference - Overview February 6th

While removing the layer, it became clear that of the approximately 10 cm applied ZBM layer at the end of the experiment, it still amounted to 5-6 cm had almost pudding-like structure, as shown in Figure 37. This figure and Figure 38 show a clear distinction between the coarse sand layer and the applied ZBM layer.

Figure 37, Large scale reference – Cross section layer build-up

Figure 38, Large scale reference – Sample layer build-up

From the 8th day (192 hours) onward, an increase in discharge was noted. Up till then, the total discharge volume was 11 litres. However, from the 8th day onward, the discharge started to increase and fluctuated between 13 and 34 l/m²/d.

5.3 COARSE LAYER

The second experiment in the first round was performed with a coarse layer on top of a sandy layer; this test started on January 18th and lasted 26 days. Similar to the tap water experiment, the water became cloudy due to applying the ZBM; however, it remained cloudy throughout the testing period.

During the application of the ZBM layer, it became clear that the coarse surface caused the ZBM layer to disintegrate into three distinguishable layers, as can be seen in Figure 39 and Figure 40. On top of the coarse sand first, a thin, darker layer settle (1), consisting of the finer sand segregated from the mixture. Subsequently, a lighter-shaded layer (2), likely a mixture of sand and bentonite, settled on top of the darker layer. Lastly, a densely clouded suspension (3) settled over time, assumably consisting of fine and lighter particles. This suspension was initially homogenous over the whole volume of water (Figure 39). However, over time, a distinction could be observed between clouded/poorly transparent and, below that, a very clouded/ not transparent suspension as a result of the settlement (Figure 40).

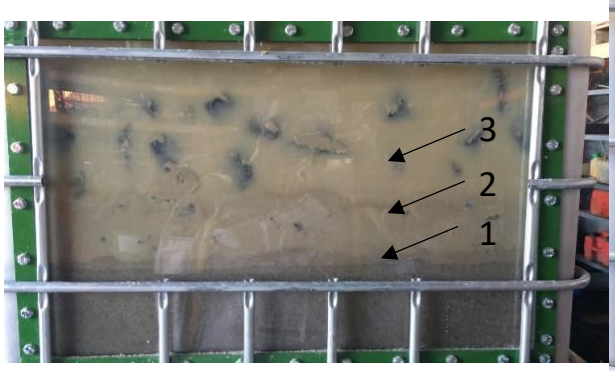

Figure 39, Large scale coarse surface – Settlement after one day

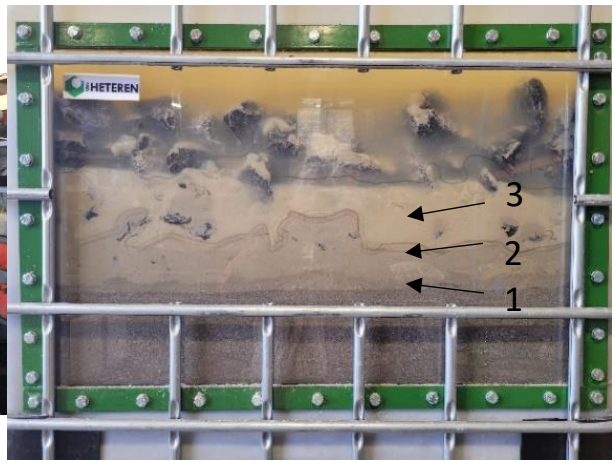

Figure 40, Large scale coarse surface - Settlement at day 22

As this container had a sight glass, it was possible to mark the layers of ZBM, which unfortunately was only done on February 1st, the 14th day of the test. Figure 40 shows the settlement over nine days. This figure shows that even after two weeks, the mixture still settles in the second and third layers, while the lowest, darker layer remains stable.

As the water was lowered at the end of the experiment, a residual amount of ZBM was observed atop the stones (Figure 41). Furthermore, during stone removal, the effect of suction was noted where stones directly interacted with the sand and bentonite, hindering the removal. Taking a sample using an electrical tube as in the reference test was difficult due to the presence of the stones; however, this resulted in a 6 cm layer of ZBM, as shown in Figure 42.

Figure 41, Large scale coarse subsurface – Water lowered

Figure 42, Large scale coarse subsurface – Sample layer build-up

In both figures regarding the discharge, it can be observed that the coarse surface overall had the most stable and the lowest discharge. The coarse surface had a maximum discharge of 0.86 l/m²/d and a lowest of 0.31 l/m²/d.

5.4 LOWERED PH

The third large-scale experiment is performed with water with a lowered pH. This water initially contained a pH of approximately 6. This experiment started on 26 February to 19 March, which is a total of 22 days. During this experiment, the water contained the same degree of turbidity throughout the experiment, as can be seen in the pictures taken on the second and 18th day of the experiment, as shown in Figure 43 and Figure 44. This turbidity made it impossible to observe the ZBM layer; even using an underwater camera, no visuals could be taken of this layer. During the removal of the water, it was impossible to get a visual of the layer due to the low transparency of the water. This resulted in only a few cm of water obstructing the view to such an extent that the ZBM layer was not visible.

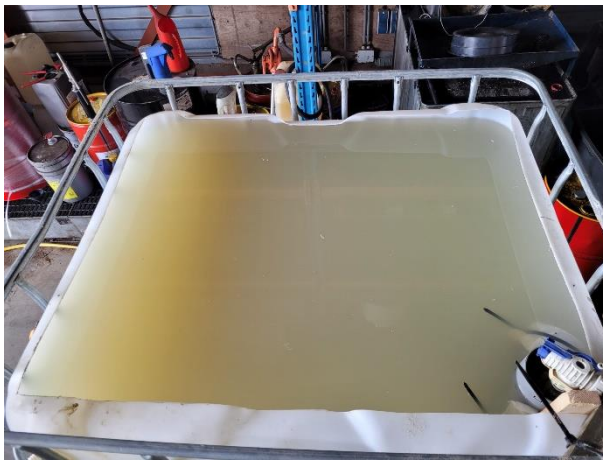

Figure 43, Large scale lowered pH - visibility day 2

Figure 44, Large scale lowered pH - visibility day 18

Through the walls, it was possible to get an idea of the ZBM layer's structure, as seen in Figure 45. In this figure, it can be seen that the ZBM layer consists of two distinctive layers, namely a darker layer (5-6 cm) and a lighter layer (1-2 cm). The lighter layer on top is assumably a result of the settlement of the finer bentonite particles facilitated by the circumstance of no river flow. It should be noted that when removing the water using the siphoning principle, this fluffy layer has also partly been removed here, indicating the low cohesion and relatively low weight of this top layer. In Figure 46, a sample is taken by using an electrical tube; this sample shows the transition between the ZBM layer and the subsurface between the 5 and 6 cm mark.

Figure 45, Large scale lowered pH - Layer build-up

Figure 46, Large scale lowered pH – Sample layer build-up

When observing the graphs with the discharge, two peaks can be noticed, which stand out in the overall trend. The first peak with pH occurred on the first day (18.6 hours), where a discharge of 13.3 l/m²/d was observed. Although both tests with salt also showed an increase in discharge, this stood out as a peak. The second peak was observed on the 11th day (258.1 hours) with a discharge of 37.31 l/m²/d. Except for these two peaks, the highest measured discharge was 4 l/m²/d.

5.5 SALINE ENVIRONMENT (NACL)

The fourth experiment was conducted with water with sodium chloride added. Due to a high discharge, this experiment ended early for the weekend because the current setup could not collect the expected amount of water. This resulted in a duration of 18 days.

Remarkable was that during this experiment, the cloudiness fluctuated. Where the initial clouded water quickly cleared up, as shown in Figure 47, which was taken one day after the experiment was started. On the eighth day, the cloudiness increased, which decreased from the 16th day. This turbidity made it impossible to take a clear photo of the crack formation from above during the experiment. These fluctuations in turbidity were not observed in any of the other experiments. During this experiment, the salt water caused an increased build-up of rust on the sight glass frame, causing an orange sheen to appear in the container.

Figure 47, Large scale NaCl - visibility after one day

Figure 48, Large scale NaCl - Occurrence of cracks during emptying of the container

Throughout the experiment, numerous cracks were observed, as shown in Figure 48 and Figure 49. In these figures, it can be seen that some cracks are more ‘’open’’ than others. This is probably related to the date of their occurrence. Where ‘’older’’ cracks had more time to close again by the supply of the looser material lying on top. Additionally, at the edge, it was observed that the ZBM layer was disconnected from the IBC container (Figure 51).

Although a self-healing process was observed, the extent of this self-healing process was limited even after stirring the water to stimulate turbulence. This turbulence was generated on the 15th day by briefly mixing the water using a concrete mixer. The stirring, along with slight tapping against the glass, caused loose material to settle in the space between the ZBM layer and the IBC container as well as in the cracks (Figure 51). The effect of stirring was noted over a subsequent period of 2 days, after which the discharge increased to its previous value, indicating a short-term and limited effect of stirring.

Figure 49, Large scale NaCl – Visual formation cracks at day 18

Figure 50, Large scale NaCl – Cross section layer structure

In addition to observing crack formation and detachment at the edges, it was noticeable that during the removal of the ZBM layer, the top layer contained chunks that were not observable in the other experiments, as shown in Figure 50. From the sample shown in Figure 52, no deviations were notable in the sample, except for the fact that the sample came out of the electric tube more easily.

Figure 51, Large scale NaCl – Detachment ZBM layer from glass

Figure 52, Large scale NaCl – Sample layer build-up

The discharge of the experiment from which NaCl is added to the water starts relatively low. However, after the weekend (day 8 (188 hours)), a steep increase in discharge was noted. Over the first measured four days, the highest discharge was 5.54 l/m²/d, whereas, from the 9th day, the discharge did not drop below 72.54 l/m²/d and peaked at 112.87 l/m²/d. Due to this high discharge at 14 days (331 hours), the mortar container and its extra overflow were both overflowed. Therefore, the total volume of water was estimated on the volume of two mortar containers as the minimum volume, which is a conservative estimate as the actual volume would likely be higher.

5.6 SALINE ENVIRONMENT ($CACL_2$)

The last experiment was conducted, exposing the ZBM to water at which 0.64 g/l $CaCl_2$ was added. This experiment was performed from 20 March to 11 April, lasting 22 days. From the start of the experiment, the water was lightly clouded, which cleared up on the second day. From the second day onward, the water had high visibility comparable to regular tap water, as seen in Figure 53.

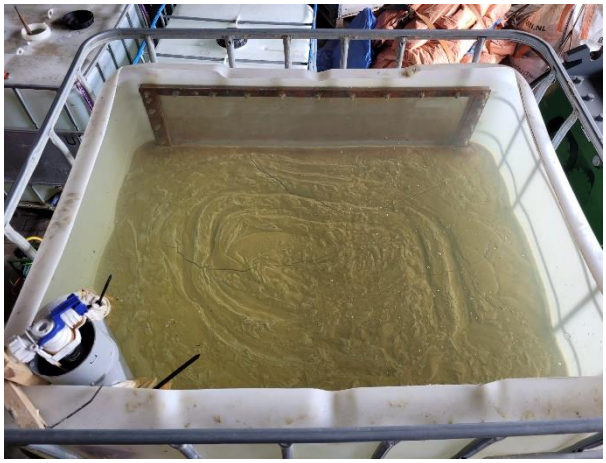

Figure 53, Large scale $CaCl_2$ – Formation cracks, day 19

Figure 54, Large scale $CaCl_2$ - Formation cracks all the way through

In Figure 53, the formation of cracks can be observed on the 19th day. After the cracks were observed, they remained stable. During the removal of the ZBM it was observed that the formations of cracks were all the way through the ZBM layer, as can be seen in Figure 54.

During the experiment, it was also noted that the ZBM layer detached around the frame of the sight glass (Figure 55). And slightly all around the border of the layer; however, the extent of detachment was less than that observed where NaCl was added in the previous experiment.

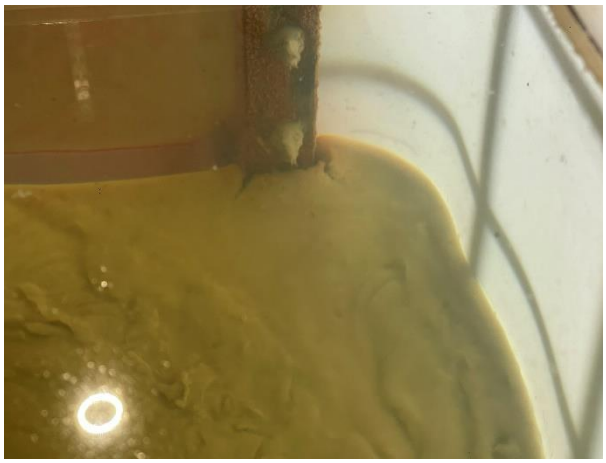

Figure 55, Large scale $CaCl_2$ - Detachment ZBM layer

Figure 56, Large scale $CaCl_2$ – Layer thickness at day 21

As the ZBM layer was removed and samples were taken, it was noticed that the ZBM layer had settled less, and a thicker remnant of the layer was observed. In the other experiments, a layer thickness between 5 and 6 cm was observed, while during this experiment, the thickness was around 7 over three samples, as shown in Figure 58.

Figure 57, Large scale $CaCl_2$ - Cross section layer structure

Figure 58, Large scale $CaCl_2$ - Sample layer build up

The discharge remained stable up till the 13th day (326 hours), where till then, the average discharge was 3.9 l/m²/d. From this day onward, the discharge started to fluctuate and increase, whereas even on the last day, a discharge of 100.3 l/m²/d was observed. On the 16th day (379 hours), the mortar container overflowed, so the discharge volume was estimated by extrapolating subsequent measurements. This was done by measuring the discharge volume 7.5 hours later, and this data was utilized to extrapolate the volume from the previous day.

5.7 KEY FINDINGS

The large-scale experiments were performed to provide insights into the influence of the various environments on hydraulic conductivity. In Table 8, an overview of the results of the large-scale experiment is shown. In this table, the hydraulic conductivity was calculated using Equation 1, the median discharge, a hydraulic head difference of 0.5 meters, and a sample length of 6 cm.

In this table, it can be seen that crack formation was observed only for the two salt concentrations. However, for the coarse surface and the lowered pH, it was not possible to observe the ZBM layer, which was not visible due to the clouded water or the presence of the coarse layer. For the discharge, it can be seen that for the lowered pH at a certain point during the experiment, the discharge was zero, indicating a completely impermeable layer. As the variation coefficient indicates, the discharges varied significantly except for the coarse surface, from which the lowest discharge was observed. Furthermore, on a large scale, the discharge of the salt environments was the highest, which is contradictory to that observed during the small-scale experiments.

Table 8, Large scale experiment - Key findings, overview results

	Duration	First Occurrence of cracks	Lowest discharge	Highest discharge	Median discharge	Total discharge	Variation coefficient	Hydraulic conductivity
Unit	***days***	***day***	***l/m²/d***	***l/m²/d***	***l/m²/d***	***l/m²***	***-***	***10^{-3} m/d***
Tap Water (Ref)	26	-	0.96	39.64	17.70	391.58	0.78	2.12
Coarse subsurface	26	Not possible	0.31	0.86	0.64	17.3	0.45	0.08
pH 6	22	Not possible	0	37.31	3.05	81.69	1.71	0.37
NaCl (8 g/l)	18	8	2.45	112.87	77.49	902.24	0.77	9.30
$CaCl_2$ (0.64 g/l)	22	15	2.17	100.3	25.89	524.32	1.03	3.11

In Table 9, an overview of the visual observations is shown for the large-scale experiments. These are divided into three characteristics: visibility, layer structure, and observations at the surface. For the visibility, it was observed that in the environment where no salt was added, the water remained clouded or took a long time to clear up. However, when salt was added, it was already possible to observe the ZBM on the second day. With respect to the formation of the layer structure, it could be observed that when the mixture is applied on top of a coarse surface, it (partially) disintegrates, causing the formation of three distinguishable layers. Furthermore, it was observed that when salt was added, the ZBM layer tended to form cracks and detaches all around, while this was not observed in the other environments.

Table 9, Large-scale experiment – Overview of visual observations during large-scale experiments

	Visibility	**Layer structure**		**Observation surface**
Tap water	Cloudy at the start, which sedimented slowly No clear visibility at the end	One layer	Cohesive	Detachment at corner
Coarse surface	Cloudy at the start, which sedimented slowly No clear visibility at the end	First darker layer	Cohesive and dense	Not observable
		Second middle layer	Cohesive	
		Third lightest layer	Fluffy	
pH neutral	Cloudy throughout	First layer	Cohesive	Not observable
		Second lighter layer	Fluffy	
NaCl (8g/l)	Cloudy fluctuates - Till day 8, clear, then decrease in visibility - On day 16, visibility increases	One layer	Highly cohesive and on top chunks	Numerous cracks observed Detachment all around
$CaCl_2$ (0.64 g/l)	Clear on the second day	One layer	Highly cohesive	Numerous cracks observed Detachment frame glass and minimal all-around

6. DISCUSSION

This chapter discusses first the limitations of the measurement methods used in the study. Next, address the influence of different environments on the experimental outcomes. Finally, it compares the results across various experimental scales, the Puls (2020) study, and standard soil types.

6.1 LIMITATIONS IN THE MEASURING METHODS

6.1.1 Limitations in the method of measuring the discharge volume

In this study, the discharge volume was measured differently for each experiment; these methods are discussed individually.

In the small-scale experiment involving a coarse surface, the discharge was measured by timing the drainage of 5 litres of water. The timing was obtained through video footage, allowing for enhanced accuracy by replaying and scrutinizing the experiment. However, the small volume of 5 litres compromises the precision of the test. Despite these factors, the obtained and converted discharge for solely coarse sand was 229.5 m/d. This result falls within the same order of magnitude as the hydraulic conductivity documented for extremely coarse sand (200 m/d) as outlined in Grondwaterformules (2024).

Another downside was that the limited water volume prevented the discharge from being measured when the ZBM was completely settled on the sandy subsurface below the coarse layer. This limitation arose from the use of a limited amount of water, resulting in a shorter timeframe for the 5 litres of water to pass through compared to the time required for the ZBM to reach the sandy subsurface. This was the result of an incorrect assessment of the behaviour of the mixture beforehand, as the first expectation was that the mixture would settle on top or within the finer grading and not all the way through.

The second small-scale experiment was similarly conducted within the 5-litre measuring cup. However, for this experiment, the discharge was deduced by measuring the lowering in water level. When the measuring cup ran dry, it would be refilled. This resulted in the water level not being the same throughout the experiment. These fluctuations in water level may give values for the discharge, which are not realistic in a real-world application due to the variations. Moreover, in a real-world application, the water level is much higher atop the ZBM layer. However, the small scale and the ease of dismantling and setting up the experiment made it possible to easily obtain initial insights into the influence of the pH and salt concentration on the mixture.

During the large-scale experiments, the discharge was measured based on the volume collected at the outflow in a mortar container, which was subsequently measured using a scale. This scale had an accuracy of 20 grams up to 10 kilograms and 50 grams above 10 kilograms. Initially, the total discharge volume would be recorded using a GoPro to make a time-lapse of the displays on the scales. This would make it possible to determine a suitable time interval afterwards based on the recordings. However, this was not possible as the scales would calibrate themselves due to the relatively slight incremental increase in weight compared to what they were designed for (weighing packages), which was contrary to the expectations, even that of the supplier. To cope with this, it was determined that the weight should be recorded manually, which was only possible on working days. As on other days, no one was present on the property of Van Heteren weg- en Waterbouw B.V. As a result, the intervals were larger than hoped, especially during the weekend, which influenced the accuracy of the trends which were based on the measured discharge volume.

Additionally, the formation and structure of the ZBM layer were assessed through observations. These observations were recorded by means of photographs, making it possible to compare them afterwards. However, the clouded water was not considered beforehand, which made it impossible to observe the formation of cracks and the structure of the layer during some of the experiments. The layer only became visible after the removal of the water.

6.1.2 Limitations in the method of measuring the pH & EC

During the experiments, the pH and EC of the water were measured. However, these measuring methods introduced limitations in the degree of certainty.

The pH measurement method involved quantifying pH in increments of 0.5 units, which limited the possibility of detecting small variations. Additionally, the pH was determined visually by applying four drops of a sample into 5 ml of solution, a process susceptible to deviations due to human error or subjective interpretation. However, prior to the experiment, the measuring method was validated by multiple times testing the pH of a bottle of water with a known pH, resulting in a similar result. Therefore, the measuring method was deemed reliable enough for the purpose of this study.

The EC was measured using an electrode, which is less prone to human errors as it could be read from a display. However, the ±100 µS/cm accuracy may have resulted in small variations captured, particularly at the lower ranges of the EC where the deviation is proportionally larger. This mainly applies when no salt was added to the water, as here the EC was in the range of 400-500 µS/cm. It also turned out during the experiments that the measurements were sensitive to stirring the water, especially in cases where salt was added, and the water had been stagnant for an extended period. This sensitivity may be attributed to the denser saltwater sinking. To mitigate the variability, all measurements were taken without stirring, possibly resulting in a lower measured EC as the heavier salt water would.

As these measuring methods only measured the pH and EC at the water's surface, it is important to consider that the actual pH and EC just above the ZBM could differ. However, these limitations are not expected to significantly impact the measurements as the measurements were primarily used to measure the course of the pH and EC. Moreover, the primary focus of this study was on measuring the total discharge volume, which is independent of the EC and pH measurements. Thus, while the limitations introduce some uncertainty regarding the water conditions, they do not influence the primary findings of the study.

6.2 INFLUENCE OF THE VARIOUS ENVIRONMENTS ON THE HYDRAULIC CONDUCTIVITY

6.2.1 Reference

In all three performed experiments, the ZBM on a sand surface with tap water acted as the reference. During the first small-scale experiment, assessing the influence of a coarse surface, the experiment with applying the ZBM on top of the sandy surface showed that applying the ZBM on top of the sand immediately reduced the discharge. This reduction was so significant that measuring how long it would take 5 litres of water to flow through the layer was not reasonably possible.

Subsequently, a small-scale experiment with the various water compositions and a large-scale experiment were performed. The small-scale tap water experiment resulted in a median discharge of 23.3 l/m²/d and the reference on a large scale of 17.7 l/m²/d. In both experiments, the discharge was initially relatively low but increased over time. As for the small scale, it started to increase on the third day after it kept fluctuating between 19.3 and 38.7 l/m²/d. Similarly, for the large scale, the discharge increased from the 8th day, from which it kept fluctuating between 12.8 and 39.6 l/m²/d. During the large-scale experiment, the increased discharge might be (partially) related to the presence of a gap between the ZBM layer and the IBC container observed on the 13th day of the experiment. This gap might have been present earlier; however, the ZBM layer was not observable due to the clouded water.

6.2.2 Influence of the coarse layer

The experiments conducted on both small and large scales aimed to assess the effectiveness of applying the ZBM atop a coarse layer in creating a poorly permeable barrier.

The small-scale experiment aimed to select a coarseness of the surface layer for the large experiment at which the mixture could settle within or on top of the coarse surface layer to form a poorly permeable layer. However, as the ZBM was applied on top of the coarse surfaces, this led to an unexpected behaviour of the ZBM. The ZBM did not tend to settle on top or within the coarse surface but would likely settle all the way through instead. However, due to experimental constraints (limited water) of the small-scale setup, it was impossible to assess if the ZBM would settle all the way through and form a poorly permeable layer.

The large-scale experiment utilised a higher water volume, making it able to measure discharge when the mixture would settle all the way through the coarse layer. Applying the ZBM on a coarse surface resulted in the lowest discharge volume and variation coefficient, indicating a low and relatively constant hydraulic conductivity. This finding is remarkable, given the initial uncertainties surrounding the behaviour and formation of the poorly permeable layer.

The lower hydraulic conductivity can likely be partially attributed to the presence of stones atop the sand, creating an impermeable barrier. Consequently, water could only infiltrate around the stones to reach the underlying sand layer, effectively reducing the actual permeable surface area. However, the influence of the presence of the stones reducing the permeable surface area is not considered the only factor reducing the discharge. The presence of the coarse layer atop the sandy subsurface would intuitively lead to a thicker ZBM layer, as the mixture would only need to fill the voids between the coarse layer whilst the volume of the mixture was kept constant, resulting in a thicker layer. Both these factors were not taken into account when determining hydraulic conductivity.

6.2.3 Influence saline environment

Small and large-scale experiments were conducted to determine whether a higher volume of total dissolved solids affects the hydraulic conductivity of the ZBM. During the small-scale and large-scale experiments, similar behaviour was observed; however, the discharge trend was significantly different. The small-scale experiment with the added salt concentration showed the lowest discharge compared to the other small-scale experiments, whereas the large scale showed the highest discharge. This high discharge is assumed to be related to the formation of cracks and the detachment of the ZBM layer from the container, which was noticed on the 8^{th} day for the NaCl and on the 19^{th} day for the $CaCl_2$ during the large-scale experiment. This extremely pronounced crack formation was not observable in the small-scale experiments, as it may be (partially) caused by the larger surface area.

The occurrence of cracks and layer detachment during the large-scale experiments is presumably due to layer shrinkage. This shrinkage may be attributed to the increased concentration of dissolved solids, which occurred in both experiments with the NaCl and $CaCl_2$ added. As in the experiment with NaCl, there is an excess of cations with a monovalent valency and in the experiment with $CaCl_2$ added, there would be an excess in divalent cations. No discrepancies were observed matching the theoretical effect of when sodium-dominated bentonite would be transformed into calcium-dominated, as described in Chapter 2.

Therefore, the shrinkage in the experiments with salt concentration is likely to be attributed to the fact that the increased salt concentration causes the shrinkage as theoretically described in Chapter 2. As the concentration of dissolved solids rises, more cations become available to neutralise negative surface charges. Consequently, the diffuse double layer's thickness decreases as the repulsive forces decrease. This causes a reduction in the volume of the bentonite up till a new equilibrium is reached between the cations present in the water between the clay platelets and its environment.

6.2.4 Influence lowered pH

During the small and large-scale experiments where the ZBM was exposed to water with a lowered pH, the objective was to assess whether the lowered pH would influence the hydraulic conductivity. However, as the higher pH of the ZBM would increase the pH of the water it was exposed to, the desired pH level of the water could not be maintained. This resulted in the experiment being performed with pH levels most of the time, similar to that of the reference experiment.

This behaviour was already noticed during the small-scale experiment where the pH of the effluent of both experiments would be 8 while the influent had a pH of 5.5 and 6.5. When setting up the large-scale experiment, this influence was considered; however, it was challenging to estimate the extent of this influence with the knowledge available. Nevertheless, the experiment was set up with the influent having a pH of 6, while the desired pH for the experiment was 7 (pH neutral). This intentionally lowered pH did not stand during the experiment as the pH did increase to 8, practically the same value as that of the reference tests. That the pH was practically the same during the large-scale experiment was also observed as the lowered pH showed very similar behaviour compared to the reference experiment. In both cases, no cracks occurred, and a similar structure of the ZBM was observed during the removal.

The fact that the pH level would increase up to a pH of 8 was not a coincidence afterwards, as the pH of solely fresh ZBM was measured once at 8 and twice at 8.5. This was measured by mixing the ZBM with a small amount of water, where the ZBM subsequently settled, and the pH of the water on top could be measured.

As during the small-scale experiment with the two lowered initial pHs, the experimental conditions were likely to be similar, the difference in discharge can not be explained. Except for the start of the experiment, the pH would likely increase to similar values within days, resulting in identical experimental conditions. The difference between a median discharge of 5.91 l/m2/d and 18.62 l/m_2/d can not be explained. Based on current insights, this can only be attributed to a certain degree of randomness that may be associated with these tests; however, as all experiments were only performed once, this cannot be validated.

As the desired pH level could not be maintained, it was not possible to assess the consequences of the lowered pH in this experiment, as the actual pH of the water was higher than intended. This would not be the case during a real-world, long-term application as, over time, the ZBM will not be able to increase the pH of the surrounding water for an extensive period and will adopt the pH of its environment; therefore, additional experiments must be performed which are able to keep a constant pH as described in the recommendations.

6.3 RESULT COMPARISON

6.3.1 Result comparison of small and large scale experiments

Table 10 and Table 11 show the median discharge and hydraulic conductivity of the small and large-scale experiments. In these tables, the hydraulic conductivity is determined using Equation 1, with two values of the sample length (L) as described later in this paragraph.

Table 10, Small scale experiment saline and lowered pH - results

	Median discharge	**Hydraulic conductivity (L=0.0228 m)**	**Hydraulic conductivity (L=0.005 m)**
Unit	***l/m²/d***	***m/d***	***m/d***
Tap water (ref)	23.28	8.85E-03	1.94E-03
Demi water	2.96	1.13E-03	2.47E-04
pH 6.5	18.62	7.07E-03	1.55E-03
pH 5.5	5.91	2.25E-03	4.92E-04
NaCl (5g /l)	1.82	6.91E-04	1.52E-04
NaCl (30 g/l)	3.95	1.50E-03	3.29E-04

Table 11, Large scale experiment - results

	Median discharge	Hydraulic conductivity (L=0.06 m)	Hydraulic conductivity (L=0.005 m)
Unit	***l/m²/d***	***m/d***	***m/d***
Tap Water (Ref)	17.70	2.12E-03	1.77E-04
Coarse subsurface	0.64	7.68E-05	6.40E-06
pH 6	3.05	3.66E-04	3.05E-05
NaCl (8 g/l)	77.49	9.30E-03	7.75E-04
$CaCl_2$ (0.64 g/l)	25.89	3.11E-03	2.59E-04

The results indicate that, while the median discharge is comparable, the hydraulic conductivity (for L=0.0228 m and L=0.06 m) differs significantly. As the experiments were conducted with different objectives and, therefore, varied in scale, this resulted in differences in key experimental characteristics. These variations are likely to influence the outcome, making it challenging to directly compare the results of the small- and large-scale experiments and translate these findings into practical applications. Ideally, to understand the influence of scale differences, the impact of key parameters should be assessed individually. However, these parameters were not individually assessed, making their influences only estimable. The main factors varying and, therefore, influencing the outcome are the ZBM layer thickness, hydraulic head difference, and surface area.

During the small-scale experiment, the ZBM layer was approximately 3.8 cm thick, whereas in the large-scale experiment, the ZBM layer was approximately 10 cm thick. Assuming the layer is homogeneous with equal hydraulic conductivity, this difference in thickness influences the volumetric discharge of water through the ZBM layer. A thicker layer would generally lead to higher total resistance and lower discharge. However, as noted by Talmon & Pennenkamp (2020), the layer is not homogeneous; the highest resistance occurs in the lowest few millimetres. Thus, the ZBM layer thickness difference likely did not significantly affect the discharge volume. This also implies that Equation 1, used to determine the hydraulic conductivity, is partly incorrect as it assumes that the resistant layer would be homogenous. For accuracy, the sample thickness in the equation should account only for the lowest millimetres of the ZBM layer, leading to much lower hydraulic conductivity. This adjustment is reflected in the hydraulic conductivity values for a 5 mm layer in Tables 10 and 11, showing a decrease in hydraulic conductivity as layer thickness decreases.

The hydraulic head difference is another factor expected to influence both discharge and ZBM behaviour. A larger hydraulic head difference results in a larger water pressure gradient, which would typically increase discharge. However, higher water pressure could also cause increased compaction, leading to a smaller void ratio and decreased hydraulic conductivity. Talmon & Pennenkamp (2020), indicated that a smaller void ratio results in larger hydraulic resistance. The relationship between these opposing processes is complex and difficult to estimate, making it challenging to provide a definitive statement based on current insights.

The last key parameter is the surface area, the surface area influences the experiment by affecting the ratio of surface area to the perimeter and the length over which shrinkage can occur. As the ratio of surface area to perimeter increases from the small to the large-scale experiment, the relative influence of the tank border decreases due to proportionally less perimeter, resulting in lower discharge. However, a larger surface area also increases the length over which shrinkage can occur, leading to longer, wider or more cracks if the tipping point is reached where the minimum stretch available is exceeded. This was substantiated by the significantly larger cracks observed in the large-scale experiments compared to the small-scale ones. This could result in cracks or the ZBM layer detaching from the container. In real-world applications, the influence of the perimeter is negligible compared to the surface area, but a larger surface area could induce crack formation due to the increased length for shrinkage.

Although the experiments were conducted with the intention of maintaining as much similarity as possible, the differing objectives between scales resulted in variations in key parameters, making direct comparisons of discharge and hydraulic conductivity across different scales impossible.

6.3.2 Results compared to that of the study by Puls

To provide an understanding of how the results of this study relate to that of the study by Puls (2020) the large-scale experiment with tap water (reference) is compared to the most comparable experiment in the study by Puls (2020), which is ‘’enkel vat 3’’. The study by Puls (2020) was conducted to provide insight into the behaviour of ZBM over the long term. An overview of the experimental conditions of this experiment and the other five experiments performed on the same scale are shown in Appendix II Table 14. Although both setups are comparable, key differences include a maintained water level difference of 1.5 meters in Puls' study, achieved through a water column above the ZBM and suction below, whereas the current study achieved only a 0.5-meter difference due to setup limitations. Puls (2020) also explored additional conditions like slopes and deliberate layer puncturing, which were not replicated here. The comparison focuses on hydraulic resistance (Equation 2), as Puls (2020) did not measure hydraulic conductivity directly.

Puls (2020) reported a hydraulic resistance of 99 days over 96 days, meeting Rijkswaterstaat’s requirement of 60 days for the Twentekanaal. The current large-scale reference test showed a hydraulic resistance of 28.3 days. The lack of self-healing observed in the current study likely contributed to this lower resistance. In practical applications, self-healing can be enhanced by turbulence and new sludge supply, as suggested by Puls (2020). The larger water level difference in Puls' study may have also contributed to a more impermeable layer and better self-healing through increased compaction and suction.

6.3.3 Results compared to that of standard soil types

To contextualize the hydraulic conductivity results (Table 11), they are compared with standard soil types (Figure 59). Without correction of the layer thickness, the highest value of the hydraulic conductivity is just in the range of clay loam, clay (poorly structured), and where most of the performed experiments resulted in a hydraulic conductivity similar to that of clay. With the correction of assuming that only a few millimetres provide the resistance, all the experiments can be categorised as dense clay based on the hydraulic conductivity.

Comparing the hydraulic conductivity of the ZBM applied on top of the coarse surface with the worst-case scenario of dense clay (hydraulic conductivity of 0.002 m/d) shows that a clay layer of 1.56 m provides a similar total hydraulic conductivity compared to that of 10 cm ZBM. This quite significant difference would result in less soil to be dredged to maintain the same water depth and therefore, assumable, less costs.

Soil type (texture)	Hydraulic conductivity (m/d)
Dense clay (no cracks, pores)	< 0.002
Clay loam, clay (poorly structured)	0.002 - 0.2
Loam, clay loam, clay (well-structured)	0.5 - 2.0
Sandy loam, fine sand	1 - 3
Medium sand	1 - 5
Coarse sand	10 -50
Gravel	100 - 1000

Figure 59, Hydraulic conductivity soil types (Ritzema & Kselik, 1996)

7. CONCLUSION

Three research questions were defined to assess the influence of various environmental factors on the hydraulic conductivity of the ZBM, with each posing its own research question. Collectively, these objectives aimed to provide deeper insights into the range of potential applications for the ZBM. Therefore, concise conclusions are drawn regarding the research questions, followed by the main objective and key findings.

1. *To what extent does the coarseness of the surface on which the ZBM is applied impact the hydraulic conductivity of the ZBM as a seepage control measure?*

Various stone gradings were assessed in the small-scale experiment, revealing that the ZBM failed to settle atop or within a coarse layer of 13.5 cm, even at the finest grading (2-8 mm). However, due to limitations in water volume, the discharge, when settled completely, could not be assessed. Large-scale experiments demonstrated that the mixture settled through the coarse layer, where, during the settlement, a partial separation of the ZBM was observed. Once settled through the coarse layer, the ZBM will form a poorly permeable layer atop the sandy subsurface.

The outcomes of the large-scale experiment indicated that the presence of the coarse layer positively influenced the formation of a poorly permeable layer in a situation without the presence of flow or turbulence. This was evidenced by the lowest median discharge and variation coefficient observed in the presence of the coarse layer compared to the other experiments.

2. *How does exposure to a higher volume of total dissolved solids (NaCl & $CaCl_2$) in the surrounding water compared to the Twentekanaal affect the hydraulic conductivity of ZBMs when used as seepage control measures?*

During both the small and large-scale experiments, it could be observed that the surface structure as a result of the application of the mixture in a salt environment, was better observable. Meanwhile, the demineralised water showed the opposite behaviour, where the sand-bentonite layer appeared flattened and fluffy. This indicates that a higher volume of dissolved solids increases the cohesion of the ZBM layer.

During the large-scale experiment, both added salt concentrations resulted in the largest discharge values and, therefore, the largest hydraulic conductivity. These large discharge values can be attributed to the consequences of shrinkage, which was not observed during the other large-scale experiments. The signs of shrinking were indicated by the formation of cracks and the detachment between the ZBM layer and the container.

The observation of shrinkage is in line with the theoretical consequence when the total concentration of dissolved solids increases, as described in Section 2.4.1. An increase in concentration of cations causes the thickness of the diffuse double layer to decrease and, therefore, the volume of the bentonite to decrease. In conclusion, as observed during the large-scale experiment, the increase in dissolved solids decreases the volume of the ZBM layer. This indirectly increases the hydraulic conductivity due to the occurrence of cracks and the detachment of the ZBM layer.

3. *What is the impact of exposing the ZBM to water with a lowered pH of the surrounding water compared to the Twentekanaal on the hydraulic conductivity of ZBMs when applied as a seepage control measure?*

The small and large-scale experiments aimed to provide insights into the impact of a lowered pH on the hydraulic conductivity of the ZBM layer. However, due to the inability to maintain the desired pH level during the experiments, the impact of lowered pH on the hydraulic conductivity of ZBMs remains unclear. Despite the intentionally lower pH of 6, while the aim was to conduct the experiment with a pH of 7, the pH quickly rose, reaching 8 by the end of the experiment due to the influence of the ZBM on the water.

As a result, no conclusion can be drawn regarding the influence of a lowered pH on the hydraulic conductivity or behaviour of the mixture. To provide insights into the influence of a lowered pH, future work should aim to maintain a constant pH. However, based on the experiments performed, as indicated by the exchange of H^+ ions, which increases the pH of the water, it can be concluded that the higher pH of the ZBM impacts the pH of its environment.

Main objective. Assessing the hydraulic conductivity of Sand Bentonite Mixture (ZBM) as a seepage reduction measure at the bottom of waterways with a coarse surface, lowered pH, and increased salt concentration of the surrounding water compared to the Twentekanaal.

Based on the experiments performed, it can be concluded that the environment influences the ZBM. Where the physical presence of a coarse surface influences the settling behaviour, resulting in a partial disintegration of the mixture while obtaining the lowest observed hydraulic conductivty. The chemical influence is indicated by the increased pH of the effluent compared to the influent as a result of an exchange of H^+ ions. Furthermore, the large-scale experiments indicated that the added salt concentration increases shrinkage resulting in a increased hydraulic conductivity. The fact that the literature can explain this observation underlines their validity.

These observations indicate the relevance of understanding the implications of diverse chemical environments on the behaviour and hydraulic conductivity of ZBMs. Apart from studies conducted explicitly for this application, existing literature primarily focuses on the influence of chemical factors on specific characteristics, such as swelling capacity, while neglecting the influence on hydraulic conductivity. This makes it very difficult to estimate the influences of various chemical environments on the hydraulic conductivity of the ZBM. Conducting experiments under various environmental conditions while measuring discharge gives better insights into the potential influence of the environment on the behaviour and hydraulic conductivity of the ZBM.

8. RECOMMENDATIONS

This chapter presents recommendations for the applicability of ZBM and future research based on the findings and limitations of the study. Recommendations are divided into subsections focusing on the experimental setup and the applicability of ZBM in various environmental conditions.

8.1 EXPERIMENTAL SETUP

As during this master's thesis, the time to assess the influence of multiple environments was limited; the choice was made to assess more environments rather than repeat the experiments. This resulted in the uncertainty not being assessed. In a follow-up study, by repeating the experiments, this degree of uncertainty could be determined.

Furthermore, the limited time also resulted in a limited duration of the experiments, resulting in the longest large-scale experiment being 26 days. To better assess the influence of the various environments, it is advisable to perform the experiment for a longer duration, ensuring that an exchange between the water and ZBM is completed, indicated by a stable environment. Consequently, it is advisable to conduct comparison experiments in future research to evaluate the influence of time on long-term behaviour and hydraulic conductivity of the ZBM layer due to environmental variations.

A factor that is not considered in this study is the influence of the hydraulic head. The pressure exerted by water atop the ZBM, coupled with the suction below, likely influences the formation and behaviour of the ZBM layer, indirectly affecting the hydraulic conductivity. To provide insight into the influence of the hydraulic head difference, additional experiments must be performed to assess the influence of the hydraulic head difference and the sensitivity of the ZBM layer to fluctuations in the hydraulic head.

Additionally, validating the hydraulic conductivity observed in scaled experiments with real-world applications would provide valuable insights, correlating experimental results with real-world applications' results.

8.2 RECOMMENDATIONS APPLICABILITY ON A COARSE SURFACE

Based on the large-scale experiment, although the results were promising, more validation is needed to conclude if ZBM can be applied on a coarse surface. The experiment suggests that when the mixture is applied to a coarse layer with 45-80 mm grading and a thickness of 35 cm, it can form a poorly permeable layer despite partial separation during settling. Provided that below the coarse layer, a fine layer is located on which the ZBM could settle.

However, as the thickness of the coarse surface increases, it is likely to affect the formation of the poorly permeable layer due to the greater degree of separation of the ZBM over a larger settling distance. The separation could cause the sand particles to settle first, reducing the relative weight of the remaining mixture. This reduction in weight increases the time it takes for the rest of the mixture to settle and raises the possibility of lighter particles being carried away by river or ship-induced flow and turbulence. Therefore, additional experiments must be performed to determine the influence of a thicker coarse layer or a different grading on the hydraulic conductivity of the ZBM layer. This experiment must be able to accommodate a thicker coarse layer, ideally replicating the intended application.

Furthermore, the presence of flow and turbulence may negatively influence the settling of the mixture, as it could cause the mixture to (partly) end up in the wrong place. Therefore, the experiment must be performed whereby flow and turbulence induced by river or ship could be simulated. These experiments could also give insights into the potential sheltering capacity of the coarse layer against flow and turbulence induced by rivers or ships.

Understanding both the influence of the coarse surface layer's thickness and grading on the ZBM layer's hydraulic conductivity, combined with the influence of flow and turbulence induced by river or ship, will provide clarity regarding the applicability in these various environments. These insights could also enhance the resilience of ZBMs against flow and turbulence from rivers or ships.

8.3 RECOMMENDATIONS APPLICABILITY IN A SALINE ENVIRONMENT

Based on the large-scale experiment, it was observed that the saline environment negatively influenced the performance of the ZBM. However, these preliminary results require further validation to draw definitive conclusions about their applicability in saline environments. Both the small and large-scale experiments focussed on assessing whether a higher concentration of dissolved solids would influence the hydraulic conductivity. During the small-scale experiment, no direct effects were observed. However, signs of shrinkage and a higher discharge were observed during the large-scale experiments. These signs of shrinkage were indicated by the formation of cracks and detachment of the sand-bentonite layer with the container.

Based on the performed test, it is unclear whether this shrinkage would also occur in the other conditions; however, it indicates that a higher concentration of dissolved solids might accelerate the occurrence of shrinkage. The shrinkage could result in the formation of cracks that, if they cannot be restored, will lead to lower resistance since the cracks are formed throughout the entire ZBM layer, as seen in the large-scale experiment. Consequently, further experiments are required to determine the influence of increased dissolved solids on hydraulic conductivity and their role in accelerating shrinkage. These additional experiments should involve identical tests conducted over an extended period with varying initial salt types and concentrations.

Furthermore, it is not possible to conclude whether sodium-dominated bentonite transforms into calcium-dominated within the limited time the experiment was performed. This would result in the platelets compacting into stacks, reducing volume, as described in Section 2.4.2. This results in decreased bentonite volume and an inability to release particles, potentially negatively affecting the ability to clog the pores and self-healing. To gain insights into this process and its consequences, an experiment must be carried out over a longer period in which the amount and type of ions between the influent and effluent are also measured. In this experiment, the concentration of calcium ions needs to be varied to see whether this would influence the exchange (rate) of sodium with calcium ions. This experiment must take place over a considerably long time (>5 months) as the low hydraulic conductivity of the ZBM potentially slows down this process.

It is important to realise that if the type and concentration of dissolved solids influence the course of the discharge, this will possibly only have negative consequences during the transition until a new equilibrium is reached in the concentration of dissolved solids. In addition, the increased concentration may only cause an accelerated transition process, which may occur in the long term in all applications where dissolved solids are present with a greater affinity, which differs from the concentration in the ZBM. Therefore, experiments with a longer duration are essential to provide insight into the transition process and the continuation of the poorly permeable layer.

8.4 RECOMMENDATIONS APPLICABILITY ENVIRONMENT WITH A LOWER PH

Based on the experiments performed, no conclusion can be made based on the influence of a lower pH on the performance of the ZBM. The inability to maintain the desired pH level during the experiments left the impact of lowered pH on the hydraulic conductivity of ZBMs unclear. However, the influence of pH on hydraulic conductivity is a factor that should not be neglected, as it could possibly decrease the critical coagulation concentration (CCC) if the pH exceeds the point of zero charge (PZC). When the CCC is surpassed, this could result in a lower swelling ability, and the bentonite starts coagulating, as explained in Section 2.5.

To properly assess the influence of lower pH on the hydraulic conductivity and behaviour of the ZBM, additional experiments should be conducted with a setup capable of maintaining a constant pH. This could be realised by a constant supply of new water, the refresh rate of which is high enough so that the influence of the ZBM on the pH could be minimised to an acceptable extent. Additionally, refreshing the water closer mimics real-world conditions as it better reflects the infinite volume of water relative to the mixture's volume over its lifetime.

9. REFERENCES

Alzamal, M., Fall, M., & Haruna, S. (2021). Swelling ability and behaviour of bentonite-based materials for deep repository engineered barrier systems: Influence of physical, chemical and thermal factors. *Journal of Rock Mechanics and Geotechnical Engineering*, 689-702.

Augustijn, D. (2023). *Reader Water Quality (course code 202300107).* University of Twente.

Bae, S., Lenhart, J. J., & Hwang, Y. S. (2021). *The effect of ionic strength, pH and natural organic matter on heteroaggregation of CeO2 nanoparticles with montmorillonite clay minerals.* Korean Society of Environmental Engineers.

Bolt, G., & Bruggenwert, M. (1978). *Soil chemistry.* Amsterdam: Elsevier scientific publishing company.

CEBO . (2024, May 21). *Dynamic Solutions, Powered By Innovation*. Opgehaald van CEBO: https://www.cebo.com/nl/oplossingen/civiele-techniek/waterput/

Christstidis, G. (2011). *The concept of layer charge of smectites and its implications for important smectite-water properties.* Chania: Department of Mineral Resources, Technical University of Crete.

Danilin, I., Tolpeshta, I., Izosimova, Y. G., Pozdnyakov, L., Stepanov, A. A., & Salimgareeva, O. (2023). *Thermal Stability and Resistance to Biodegradation of Humic Acid Adsorbed on Clay Minerals.* Moscow: Lomonosov Moscow State University.

Dickson, A. G., & Goyet, C. (1994). *Handbook of methods for the analysis of the various parameters of the carbon dioxide system in sea water.*

Dutta, J., & Mishra, A. (2016). Consolidation behaviour of bentonites in the presence of salt solutions. *Elsevier*, 61-69.

Farrar, J. (2004). *Guidelines for Performing Foundation Investigations for Miscellaneous Structures.* Denver: United States Department of the Interior.

Ghaedi, M. (2021). *Adsorption: Fundamental Processes and Applications.* Elsevier: Yasouj.

Grondwaterformules. (2024, Januari 11). *doorlatendheid k*. Opgehaald van grondwaterformules.nl: http://grondwaterformules.nl/index.php/vuistregels/ondergrond/doorlatendheid-per-grondsoort

Hofkamp, J. (1986). *Zand-betoniet mengsel als afdichtigsmateriaal voor vuilstortplaatsen.* Wageningen: Wageningen Universiteit & Research centre.

Keerthana, S., & Arnepalli, D. N. (2022). Hydraulic Performance of Polymer-Modified Bentonites for Development of Modern Geosynthetic Clay Liners: A Review. *International Journal of Geosynthetics and Ground Engineering*.

Kim, D. (2003). *Mesurement of point of zero charge of bentonite by solubilization technique and its dependence of surface potential on pH.* Seoul: Department of Environmetal Science and Engineering, Ewha Womans University.

Kong, D.-J., Wu, H.-N., Chai, J.-C., & Arulrajah, A. (2017). *State-Of-The-Art Review of Geosynthetic Clay Liners.*

Li, Z., Su, G., Zheng, Q., & Nguyen, S. T. (2020). A dual-porosity model for the study of chemical effects on the swelling behaviour of MX-80 bentonite. *Acta Geotechnica*, 635-653.

Manca, D., Ferrari, A., & Laloui, L. (2015). Fabric evolution and the related swelling behaviour of a sand/bentonite mixture upon hydro-chemo-mechanical loadings. *Géotechnique*, 1-17.

Mitchell, J. K., & Soga, K. (1993). *Fundamentals of Soil Behavior.* Wiley.

Nasir, O., Nguyen, S. T., Barnichon, J.-D., & Millard, A. (2017). Simulation of the hydro-mechanical behaviour of bentonite seals for the containment of radioactive wastes. *Canadian Geotechnical Journal*, 1055-1070.

Neretnieks, I., Liu, L., & Moreno, L. (2009). *Mechanisms and models for bentonite erosion.* Stockholm: Royal Institute of Technology, KTH.

Nortier, I., & de Koning, P. (1991). *Hydraulica voor waterbouwkundigen.* Houten: Educatieve partneres Nederland BV.

Oliveira, A., & Beatrice, C. (2019). *Polymer Nanocomposites with Different Types of Nanofilter.* IntechOpen.

Olsthoorn, T. N. (2020). *Essentieel gedrag van Na-bentoniet en van Ca-bentoniet na beslibbing van bodem van een kanaal met zoet water.*

Prioa, R., Croce, P., & Modoni, G. (2016). Experimental investigation of compacted sand-bentonite mixtures. *Elsevier*, 51-56.

Puls, A. (2020). *Beslibbingsonderzoek.* Van Heteren Weg- en Waterbouw B.V.

Qin, Y., Xu, D., & Lalit, B. (2021). Effect of bentonite content and hydration time on mechanical properties of sand bentonite mixture. *Applied sciences*.

Rehab, A. (2013). *Numerical studies of piles in saturated expanisve soil.* Structural Engineering Department Faculty of Engineering Zagazig University.

Rijkswaterstaat. (2021). *Oplegnotitie onderzoeksrapporten Zand-Bentoniet.* Rijkswaterstaat.

Rijkswaterstaat. (2023, November 7). *Twentekanaal*. Opgehaald van Rijkswaterstaat: https://www.rijkswaterstaat.nl/water/vaarwegenoverzicht/twentekanalen

Rijkswaterstaat. (2024, February 21). *Rijkswaterstaat Waterinfo*. Opgehaald van waterinfo.rws: https://waterinfo.rws.nl/#/nav/expert

Ritzema, H., & Kselik, R. (1996). *Drainage of irrigated lands.* Rome: Food and agriculture organization of the united nations.

Robinson, R., & Allam, M. (1998). Effect of Clay Mineralogy on Coefficient of Consolidation. *Clays and Clay minerals*, 596-600.

Sällfors, G., & Öberg-Högsta, A.-L. (2002). *Determination of hydraulic conductivity of sand-bentonite mixtures for engineering purposes.* Goteborg: Department of Geotechnical Engineering, Chalmers University of Technology.

Shaw, E. M., Beven, K. J., Chappell, N. A., & Lamb, R. (2011). *Hydrology in Practice.* Abingdon: Spon Press.

STOWA. (2024, February 23). *Brakke wateren*. Opgehaald van STOWA: https://www.stowa.nl/deltafacts/waterkwaliteit/kennisimpuls-waterkwaliteit/brakke-wateren

Studds, P., Stewart, D., & Cousens, T. (1998). The effect of salt solutions on the properties of bentonite-sand mixtures. *The Mineralogical Society*, 651-660.

Talmon, A., & Pennekamp, J. (2020). *Geotechnische en geochemische proeven t.b.v. Twentekanalen.* Deltares.

Taylor, R., & Smith, T. (2017). The engineering geology of clay minerals; swelling, shrinking and mudrock breakdown. *Mineralogical Society of Great Britain and Ireland*, 235-260.

Tu, H. (2015). *Prediction of the variation of swelling pressure and 1-D heave of expansive soils with respect to suction.* Ottawa: Faculty of Engineering University of Ottawa.

Wayllace, A. (2008). *Volume change and swelling pressure of expansive clay in the crystalline swelling regime.* University of Missouri .

10. APPENDIX

10.1 APPENDIX I: SUBSTANTIATION OF INITIAL CONDITIONS LARGE-SCALE EXPERIMENT

10.1.1 Substantiation pH

Although no future normative scenarios have been looked into while determining the concentrations, historical data will be used to base the analysis on a realistic scenario. This historical data shows an average pH of 7.9 and a standard deviation of 0.27 of the 22 locations over a period of 10 years, as shown in Appendix I (Table 12). Additionally, in this table, a significant difference can be seen between the lowest (6.3) and highest (9.1) observed pH over all the locations and the location with the largest differences between the lowest (6.3) and highest (8.6) is at the Twentekanaal near Enschede. This shows the wide variety in pH values to which the ZBM could be exposed to.

Since the desire was to perform this test only once, it was decided to expose the bentonite sand to a pH of 7. However, to cope with the influence of the ZBM on the water, the initial pH will be 6. This somewhat extreme value considers that the ZBM will increase the pH to a certain extent, as observed in the small-scale experiment. However, it is expected that as the water volume ratio to the surface area increases, the influence of the ZBM decreases. This extent is difficult to predict, and the actual pH value must be evident from the effluent. The initial pH of 6.0 was achieved by adding pH minus into an IBC container filled with softened tap water.

Table 12, pH value and Cl concentration Netherlands (Rijkswaterstaat, 2024)

		pH							Cl (mg/l)						
Observation point	Waterway	Num obs	Q0	Q1	Q2	Q3	Q4	Average	Num obs	Q0	Q1	Q2	Q3	Q4	Average
Almelo	Twentekanaal	129	6,5	7,6	7,9	8,1	8,7	7,8	130	31,0	56,4	65,7	77,5	126,0	68,1
Amsterdam (kilometer 25, IJtunnel)	Het IJ	143	7,5	7,8	7,9	8,0	8,4	7,9	143	390,0	1635,0	2300,0	2955,0	4530,0	2280,3
Belfeld boven	Maas	130	6,5	7,8	7,9	8,0	8,7	7,9	130	14,0	28,9	40,3	51,8	75,9	41,2
Bocht van Watum	Eems	189	7,5	8,0	8,1	8,1	8,8	8,0	120	6540,0	10000,0	11950,0	13000,0	18300,0	11575,3
Bovensluis	Hollands diep	129	7,5	8,0	8,1	8,2	8,8	8,1	130	29,0	58,0	70,0	84,0	141,0	71,2
Eefde boven	Twentekanaal	123	6,9	7,6	7,8	7,9	8,4	7,8	124	15,1	43,7	54,4	70,7	122,0	59,0
Eemmeerdijk, kilometer 23	Eemmeer	128	7,3	8,0	8,2	8,3	9,1	8,2	128	53,0	74,4	80,0	90,1	120,0	82,7
Enschede Vitens	Twentekanaal	129	6,3	7,5	7,6	7,8	8,6	7,6	130	29,0	55,0	78,0	95,9	141,0	77,3
Genemuiden	Zwartewater	130	6,9	7,5	7,7	7,8	9,1	7,7	129	33,0	47,8	54,0	65,5	103,0	57,5
Gouda voorhaven	Hollandsche Ijsel	128	6,5	7,6	7,8	7,9	8,5	7,7	128	47,0	96,6	120,0	140,3	280,0	125,2
Innamewerk Water Productiebedrijf Heel	Maas	102	7,2	7,7	7,8	7,8	8,1	7,8	116	22,0	31,8	42,8	55,0	79,0	43,2
Keizersveer	Bergschemaas	122	7,2	7,9	7,9	8,0	9,1	8,0	121	21,9	34,8	43,0	57,5	76,0	45,7
Lobith ponton	Boven Rijn	261	7,7	7,9	8,0	8,1	8,5	8,0	261	32,8	66,9	78,4	92,0	170,0	80,0
Maassluis	Nieuwe Waterweg	141	6,4	8,0	8,0	8,1	8,4	8,0	142	69,0	959,5	1530,0	2487,5	7000,0	1827,6
Nederweert	Zuid Willemsvaart	130	7,4	7,7	7,8	8,0	8,6	7,8	0						
Nieuwegein	Lekkanaal	129	7,7	8,1	8,1	8,2	8,4	8,1	129	40,0	66,0	73,0	79,0	120,0	73,1
Nieuwersluis	Amsterdam-Rijnkanaal	130	7,4	8,0	8,0	8,1	8,2	8,0	130	44,0	65,0	71,0	79,0	125,0	73,0
Sas van Gent	Kanaal Gent naar Terneuzen	125	7,0	7,8	7,8	7,9	8,2	7,8	129	181,0	971,0	1750,0	2780,0	6000,0	2165,7
Stevensweert	Maas	131	7,3	7,8	7,9	8,0	8,6	7,9	0						
Terneuzen boei 20	Westerschelde	126	7,7	8,0	8,0	8,1	8,1	8,4	131	10000,0	12750,0	13800,0	15000,0	19100,0	13772,5
Westzaan (kilometer 13)	Noordzeekanaal	195	7,1	7,7	7,8	7,9	8,3	7,8	195	1400,0	3345,0	4090,0	4995,0	6500,0	4094,3
Wiene	Twentekanaal	129	6,7	7,5	7,7	7,9	8,5	7,7	130	35,0	53,0	66,0	81,5	119,0	68,1
Average				7,1	7,8	7,9	8,0	8,6	7,9		951,3	1521,9	1817,8	2116,9	3161,4	1834,0
Largest difference				1,4	0,6	0,5	0,5	1,0	0,6		9986,0	12721,2	13759,8	14948,2	19024,1	13731,4

10.1.2 Substantiation sodium concentration

Similarly, the added salt concentrations are based on a similar methodology, which makes use of the chloride and sodium concentrations in the surface water. In Appendix I (Table 12), the chloride (mg/l) concentration and in Appendix II (Table 13), the Sodium concentration is shown over a period from 2013 to 2022 and 20 locations. These tables show significant variability probably caused by the supply of saltwater, making it difficult to determine a representative sodium chloride concentration.

Based on the chloride concentration, the water can be categorised into five categories. Up to 300 mg/l as freshwater, 300-1000 mg/l slightly brackish, 1000-3000 mg/l weakly brackish and from 3000-10000 mg/l brackish to salt and above 10000 mg/l as salt water. Currently, there is no desire to apply the ZBM to a brackish-to-salt environment, so the effect of the chloride concentration higher than 3000 mg/l is not considered (STOWA, 2024).

However, as can be seen in Appendix I (Table 12), the chloride concentration may fluctuate quite heavily. For example, at Sas van Gent, the average chloride concentration is 2166 mg/l, and the highest observed value is 6000 mg/l. To the same extent, the sodium concentration fluctuates as at Kanaal Gent-Terneuzen near Sas van Gent; the average is 1195 mg/l, and the maximum is 3320 mg/l. This shows the difficulties of choosing one representative concentration, which will result in a valuable experiment.

Natrium chloride concentration (NaCl) added to water is determined first based on sodium concentration using Equation 3. The maximum concentration observed at Sas van Gent was used as a reference sodium concentration.

$$\frac{CNa}{MNa} * (MCl + MNa) \tag{3}$$

$CNa = Concentration\ sodium\ \left(\frac{g}{l}\right)$

$MNa = Molar\ mass\ sodium\ \left(\frac{g}{mol}\right)$

$MCl = Molar\ mass\ chloride\ \left(\frac{g}{mol}\right)$

$$= \frac{3.320}{22.99} * (35.45 + 22.99) = 8.44\ g/l\ NaCl$$

Equation 3, Mass NaCl per litre

The sodium chloride concentration is also validated using Sas van Gent's maximum observed chloride concentration. However, first, the ratio of chloride particles in seawater originating from sodium chloride is determined by using the molality of sodium and chloride in seawater, resulting in a ratio of 0.860. Assuming that all sodium particles originate from NaCl, however, not all chloride particles originate from NaCl. The ratio of chloride particles originating from NaCl is determined by dividing sodium's molarity by chloride (Dickson & Goyet, 1994).

This ratio is then multiplied by the maximum observed chloride concentration (6000 mg/l), resulting in an estimated 5160 mg/l of chloride bonded with sodium. Although the chloride concentration exceeds the set limit of 3000 mg/l for weakly brackish water, it is considered representative due to significant fluctuations. Subsequently, by making use of Equation 3, however, instead of dividing the concentration of sodium by the molar mass of sodium, this is done with the concentration of chloride and molar mass of chloride, resulting in a mass NaCl of 8.54 g/l, corresponding to the calculated concentration of NaCl based on sodium concentration.

However, as the sodium chloride is supplied in 25 kg bags, it was decided to lower the concentration to 8 g/l so that a total of 3 m3 of salt water could be produced during the experiments using 25 kg salt. This concentration is similar to a sodium concentration of 3150 mg/l and chloride concentration of 4850 with a ratio of 0.86 included.

10.1.3 Substantiation calcium concentration

The determination of the calcium concentration is similar to that of the sodium concentration and pH, namely looking at the observed data shown in Table 13. While calcium levels exhibit some variability, they remain more stable compared to sodium and chloride concentrations. Notably, similar locations with higher sodium concentrations also exhibit higher calcium concentrations, indicating a relationship with the influence of seawater.

Calcium dichloride ($CaCl_2$) is added to replicate this calcium concentration as $CaCl_2$ is better soluble than $CaCO_3$ (calcium carbonate) and is more common in the literature. For example, the study of Dutta & Mishra (2016) compared the effect of varying NaCl and $CaCl_2$ concentrations on the consolidation behaviour of compacted bentonites.

To determine the calcium concentration, the same normative location used to determine the sodium concentration is used, Sas van Gent. At this location, the maximum observed concentration is 230 mg/l. There is only one more extreme location, which is at the Westerschelde; this location is not considered, as it could be defined as a saltwater environment (Cl concentration >10000 mg/l). The calcium dichloride concentration is calculated using Equation 3, which resulted in an added concentration of 0.64 g/l.

Table 13, Na and Ca concentration Netherlands (Rijkswaterstaat, 2024)

		Na (mg/l)								Ca (mg/l)							
Observation point	Waterway	Num obs	Q0	Q1	Q2	Q3	Q4	Average		Num obs	Q0	Q1	Q2	Q3	Q4	Average	
Almelo	Twentekanaal	128		21,8	38,5	44,0	53,0	73,0	45,1	128		35,0	52,0	59,0	68,1	100,0	60,0
Amsterdam (kilometer 25, IJtunnel)	Het IJ	143		230,0	966,5	1400,0	1700,0	2500,0	1319,7	143		79,0	98,1	110,0	124,5	210,0	111,4
Belfeld boven	Maas	128		11,0	19,6	30,9	41,3	59,0	31,5	128		38,8	58,0	63,0	66,0	77,0	61,8
Bocht van Watum	Eems	0															
Bovensluis	Hollands diep	115		17,5	31,8	39,0	47,0	78,0	39,8	115		50,0	61,8	66,0	70,0	85,0	66,1
Eefde boven	Twentekanaal	122		11,0	28,0	35,6	42,8	74,0	36,8	122		41,0	70,0	76,5	84,0	96,0	76,4
Eemmeerdijk, kilometer 23	Eemmeer	126		33,0	45,0	49,2	55,8	82,0	50,6	126		38,0	51,9	61,3	68,7	98,0	60,8
Enschede Vitens	Twentekanaal	128		18,2	33,3	48,5	61,2	110,0	49,5	128		29,0	42,8	46,0	49,0	63,4	45,5
Genemuiden	Zwartewater	130		19,8	30,0	35,0	45,0	64,0	37,7	130		38,6	60,0	64,4	68,4	78,0	63,3
Gouda voorhaven	Hollandsche IJsel	128		33,0	55,9	66,0	78,5	144,0	70,6	128		57,0	71,6	80,5	93,1	120,0	83,3
Innamewerk Water Productiebedrijf Heel	Maas	127		13,0	20,0	27,4	38,0	58,0	29,6	127		42,0	59,0	66,2	71,6	85,0	65,1
Keizersveer	Bergschemaas	120		11,0	22,0	29,8	40,1	57,7	31,2	120		42,0	54,0	59,0	63,0	76,0	58,4
Lobith ponton	Boven Rijn	258		18,0	35,0	42,0	51,0	110,0	44,2	258		54,0	64,2	68,8	73,8	88,0	69,2
Maassluis	Nieuwe Waterweg	142		39,6	569,3	880,0	1400,0	3800,0	1067,9	143		45,0	86,5	99,0	118,0	200,0	103,4
Nederweert	Zuid Willemsvaart			13,0	23,0	30,7	41,7	71,0	33,4			43,0	60,4	66,3	72,9	84,0	66,1
Nieuwegein	Lekkanaal	129		23,0	36,0	40,3	44,8	68,6	40,8	129		54,6	62,6	66,5	70,9	81,2	67,0
Nieuwersluis	Amsterdam-Rijnkanaal	117		26,3	37,1	41,0	45,6	71,5	41,7	117		54,2	63,6	68,3	72,4	82,8	68,4
Sas van Gent	Kanaal Gent naar Terneuzen	128		95,0	536,8	991,0	1600,0	3320,0	1195,4	128		103,0	135,8	145,0	160,0	230,0	151,3
Stevensweert	Maas	116		10,0	17,6	27,1	38,8	65,0	30,2	116		38,7	60,0	67,0	75,0	89,0	67,0
Terneuzen boei 20	Westerschelde	131		5910,0	7300,0	8200,0	8605,0	10000,0	8048,6	131		258,0	319,5	350,0	370,0	450,0	348,1
Westzaan (kilometer 13)	Noordzeekanaal	206		487,0	1900,0	2300,0	2800,0	4100,0	2327,0	206		106,0	132,0	150,0	160,0	200,0	147,1
Wiene	Twentekanaal	3		14,1	35,1	43,0	53,1	84,0	44,9	3		36,2	50,3	57,1	69,0	110,0	60,0
Average				57,3	224,0	310,0	413,9	749,5	328,4			61,1	81,6	90,0	98,5	128,7	90,5
Largest difference				477,0	1882,4	2273,0	2762,0	4042,3	2297,4			229,0	276,8	304,0	321,0	386,6	302,6

10.2 APPENDIX II: RESULTS PULS (2020)

Table 14, Hydraulic resistance (Mediane weerst (d)) and characteristics of the tests carried out in the IBC containers by Puls (2020)

Proef	Enkel vat 1	Enkel vat 2	Enkel vat 3	Dubbel vat 1	Dubbel vat 2	Dubbel vat 3
Start	15-11-2019	14-01-2020	09-03-2020	10-12-2019	09-03-2020	15-05-2020
Eind	10-01-2020	24-02-2020	12-6-2020	14-02-2020	12-05-2020	15-6-2020
Duur [dagen]	57 d	42 d	96 d	77 d	65 d	30 d
Zand [vol %]	30%	20%	25%	30%	25%	25%
Korreldiam toegevoegd zand	Zie bijl. voor zeefkromme	Zie bijl. voor zeefkromme	Zie bijl. voor zeefkromme	Zie bijl. voor zeefkromme	Zie bijl. voor zeefkromme	Zie bijl. voor zeefkromme
Bentoniet	Na-RONA aangeleverd door leverancier "bentoniet 1"	Na-RONA aangeleverd door leverancier "bentoniet 2"	OCMA poeder aangeleverd door CEBO & zelf aangemaakt met venturi-hopper	Na-RONA aangeleverd door leverancier "bentoniet 1"	OCMA poeder aangeleverd door CEBO & zelf aangemaakt met venturi-hopper	OCMA poeder aangeleverd door CEBO & zelf aangemaakt met venturi-hopper
Viscositeit [s/L]	120 s/L	120 s/L	120 s/L	120 s/L	120 s/L	120 s/L
Water	Onthard leidingwater	Onthard leidingwater	Kanaalwater bij bedrijf	Onthard leidingwater	Kanaalwater bij bedrijf	Kanaalwater bij bedrijf
Afvoer	Buis loopt vrij uit	Buis in overloopvat	Buis in overloopvat	Buis in overloopvat	Buis in overloopvat	Geen of buis in overl. vat
Drukval [m]	1,5 m	1,5 m	1,5 m	1,5 m	1,5 m	0-1,5 m
Talud	1:6	1:6	geen	1:6	1:6	1:6
Vat						
Lengte [m]	1,10 m	1,10 m	1,10 m	2,00 m	2,00 m	2,00 m
Breedte [m]	0,95 m	0,95 m	0,95 m	0,95 m	0,95 m	0,95 m
Hoogte [m]	1,00 m	1,00 m	1,00 m	1,00 m	1,00 m	1,00 m
Scheuren?	Ja	Ja	Ja	Ja	Ja	Ja
Bentoniet Batchnr.	OCMA onbekend	OCMA onbekend	OCMA bekend	OCMA onbekend	OCMA bekend	OCMA bekend
Mediane weerst. [d]	69 d	270 d	99 d	290 d	18 d (slecht herstel gaten boven in talud)	n.v.t. (geen doorstroming)
Grafieken debiet [mm/uur]	Figuur 22 p43/44	Figuur 55 p84	Figuur 93 p119/120	Figuur 37 p62/63	Figuur 71 p97/98	n.v.t.
Grafieken weerst. [d]	Figuur 23 p45/46	Figuur 56 p85	Figuur 94 p121/122	Figuur 38 p64/65	Figuur 72 p99/100	n.v.t.